# Fresh-water and salt-water distribution in passive margin sediments: Insights from Integrated Ocean Drilling Program Expedition 313 on the New Jersey Margin

**Johanna Lofi[1,*], Jennifer Inwood[2,*], Jean-Noël Proust[3,*], Donald H. Monteverde[4,5,*], Didier Loggia[1,*], Christophe Basile[6,*], Hironori Otsuka[7,*], Takeshi Hayashi[8,*], Susanne Stadler[9,*], Michael J. Mottl[10,*], Annick Fehr[11,*], and Philippe A. Pezard[1,*]**

[1]*Geosciences Montpellier, UMR5243, Bâtiment 22, Université Montpellier 2, 34095 Montpellier cedex 5, France*
[2]*Department of Geology, University Road, University of Leicester, Leicester LE1 7RH, UK*
[3]*UMR 6118 CNRS Géosciences, Université de Rennes 1, 35042 Rennes cedex, France*
[4]*Department of Earth and Planetary Sciences, Rutgers University, Piscataway, New Jersey 08854, USA*
[5]*New Jersey Geological Survey, PO Box 427, Trenton, New Jersey 07640, USA*
[6]*ISTerre, Université Joseph Fourier, BP 53, 38041 Grenoble CEDEX 9, France*
[7]*Ocean Research Institute, University of Tokyo, Ocean Floor Geoscience, 1-15-1 Minamidai, Nakanoku, Tokyo, Japan*
[8]*Akita University, Tegata-gakuen-mach, Akita 010-850 2, Japan*
[9]*Federal Institute for Geosciences and Natural Resources (BGR), Stilleweg 2, 30655 Hannover, Germany*
[10]*Department of Oceanography, University of Hawaii, 1000 Pope Road, Honolulu, Hawaii 96822, USA*
[11]*GGE, E.ON Energy Research Center, RWTH Aachen University, Mathieutsrasse 10, D-52074 Aachen, Germany*

## ABSTRACT

**On the New Jersey shelf (offshore North America), the presence of pore water fresher than seawater is known from a series of boreholes completed during the 1970s and 1980s. To account for this fresh water, a first hypothesis involves possible present-day active dynamic connections with onshore aquifers, while a second involves meteoritic and/or sub–ice-sheet waters during periods of lowered sea level. Expedition 313 drilled three boreholes on the middle shelf, offering a unique opportunity for the internal structure of the siliciclastic system to be accessed, at scales ranging from the depositional matrix to the continental margin. This enables the stratigraphic architecture to be correlated with the spatial distribution and salinity of saturating fluids. Expedition 313 revealed both very low salinities (<3 g/L) at depths exceeding 400 m below the seafloor and evidence for a multilayered reservoir organization, with fresh- and/or brackish-water intervals alternating vertically with salty intervals. In this study we present a revised distribution of the salinity beneath the middle shelf. Our observations suggest that the processes controlling salinity are strongly influenced by lithology, porosity, and permeability. Saltier pore waters generally occur in coarse-grained intervals and fresher pore waters occur in fine-grained intervals. The transition from fresher to saltier intervals is often marked by cemented horizons that probably act as permeability barriers. In the lowermost parts of two holes, the salinity varies independently of lithology, suggesting different mechanisms and/or sources of salinity. We present an interpretation of the sedimentary facies distribution, derived from core, logs, and seismic profile analyses, that is used to discuss the margin-scale two-dimensional reservoir geometry and permeability distribution. These proposed geometries are of primary importance when considering the possible pathways and emplacement mechanisms for the fresh and salty water below the New Jersey shelf.**

*Emails: Lofi: johanna.lofi@gm.univ-montp2.fr; inwood: ji18@leicester.ac.uk; Proust: jean-noel.proust@univ-rennes1.fr; Monteverde: dmonte@rci.rutgers.edu; Loggia: loggia@univ-montp2.fr; Basile: cbasile@ujf-grenoble.fr; Otsuka: otsuka@ori.u-tokyo.ac.jp; Hayashi: thayashi@ed.akita-u.ac.jp; Stadler: Susanne.Stadler@bgr.de; Mottl: mmottl@soest.hawaii.edu; Fehr: Annick.Fehr@eonerc.rwth-aachen.de; Pezard: ppezard@gulliver.fr.

## INTRODUCTION

Many passive continental margins are characterized by high sedimentation rates and are thus good indicators of the past climatic, eustatic, and sedimentary flux changes. Due to their architecture and sediment composition, these margins are capable of accommodating good reservoirs, generally studied offshore for hydrocarbon purposes. It has been known for some time that such margins can also contain a large amount of fresh water (Cohen et al., 2010; Hathaway et al., 1979; Kohout et al., 1977), part of which can be released to the ocean via submarine groundwater discharge (Taniguchi et al., 2002). With more than 30% of the world population living in coastal areas, such systems are clearly of high interest for determining and managing viable water resources (Barlow, 2003; Bear et al., 1999). Moreover, they are the site of chemical exchanges between the continental and marine domains (Bugna et al., 1996; Burnett et al., 2001; Groen et al., 2000) and, as such, could be directly implicated in geochemical balances between ocean, atmosphere, and biosphere reservoirs (Faure et al., 2002; Taniguchi et al., 2002).

Fresh-water reservoirs are of clastic (carbonate and terrigenous), karstic, or fractured origin. Clastic continental aquifers are easily identified and many are exploited for societal purposes (Barlow, 2003). On passive margins, they are known to generate subsurface fresh-water fluxes toward the oceans. As they generally extend offshore, they are prone to seawater intrusion. Offshore, they form complex systems and their dynamics remain poorly known. Brackish to fresh waters have been found in boreholes

*Geosphere*; August 2013; v. 9; no. 4; p. 1009–1024; doi:10.1130/GES00855.1; 5 figures; 3 tables.
Received 4 August 2012 ♦ Revision received 13 February 2013 ♦ Accepted 1 July 2013 ♦ Published online 16 July 2013

several kilometers away from the coastline on the continental shelves and upper slopes (Austin et al., 1998; Hathaway et al., 1979; Scientific Committee on Oceanic Research, Land-Ocean Interactions in the Coastal Zone, 2004; Kohout et al., 1977; Malone and Martin, 2000; Manheim and Paull, 1981). In carbonate environments, offshore exploratory drillings have identified fresh waters (salinity < 1 g/L) in deep karstic cavities (Scientific Committee on Oceanic Research, Land-Ocean Interactions in the Coastal Zone, 2004; Vernet, 2000). In siliciclastic environments, fresh waters (salinity < 3 g/L) have been recognized as deep as 400 m below the seafloor (mbsf) on the New Jersey Margin, in Miocene successions (Mountain et al., 2010). The volume of fresh water stored in passive margins worldwide is estimated to be $3 \times 10^5$ $km^3$ (Cohen et al., 2010).

Coastal hydrogeologists and oceanographers recognize the significant contribution that submarine groundwater discharge could make to the coastal ocean (Taniguchi et al., 2002); offshore, some of these discharges have been detected at water depths of several hundred meters (Robb, 1984; Dugan and Flemings, 2000; Fleury et al., 2007; Salvati and Sasowsky, 2002). Sinkholes in carbonates have been imaged, sometimes associated with active resurgences (Land and Paul, 2000; Lofi et al., 2012; Swarzenski et al., 2001). The amount of expulsed water from the world margins could compose as much as 10% of the total river flow to the ocean (Taniguchi et al., 2002). These water transfers may be both volumetrically and chemically important to coastal water and chemical budgets. In some places, water expulsion associated with submarine groundwater discharge also represents a risk to continental slope stabilities (Dugan and Flemings, 2000) with consequences to anthropogenic installations (Sultan et al., 2001).

Two main hypotheses might explain the presence of fresh water in New Jersey offshore reservoirs. The first involves possible present-day active dynamic connections with onshore aquifers (van Geldern et al., 2013), and the second involves meteoritic and/or sub–ice-sheet waters recharged during lowered sea-level periods (Cohen et al., 2010; Kooi and Groen, 2001; Person et al., 2003). Data from the field that would allow hypotheses to be tested is currently lacking and the study of offshore fresh-water reservoirs and their associated onshore-offshore groundwater flow dynamics at the margin scale remains a challenge. Offshore field data are scarce because they require technically difficult and expensive drilling operations, in the best cases gathering only indirect data (e.g., seismic or resistivity profiles). In clastic systems, the sampling is often challenging, and core recovery low, due to the poor consolidation of the sediments and overpressured horizons. Difficulties increase in carbonate sediments where karstic networks are uneven and their geometries unpredictable. The offshore characteristics of fresh-water reservoirs on passive margins are therefore poorly constrained. Understanding the architecture, history, and dynamics of fresh-water submarine reservoirs is emerging as a new scientific frontier to assess the dynamics of groundwater exchanges between the continental and oceanic reservoirs.

Offshore groundwater circulations at the margin scale are generally studied using analytical and numerical models. Geochemical studies performed near submarine seeps or from borehole samples and geophysical investigations remain rare. However, defining an accurate reservoir architecture and heterogeneity at the scale of the margin is of primary importance for providing coherent conceptual geological models, which can lead to better predictions of preferential past and present-day flow pathways (Bowling et al., 2005; Cohen et al., 2010; Marksamer et al., 2007). In this context, this study focuses on borehole data from three sites drilled during Integrated Ocean Drilling Program Expedition 313 in sediments from the shallow inner shelf of the New Jersey clastic passive margin. The excellent core recovery (>80%) through the targeted Miocene successions combined with the acquisition of geophysical data (wireline logs and core petrophysical data) offers a unique opportunity to access the internal structure of a siliciclastic system, at scales ranging from the matrix to the margin. This has enabled the construction of a two-dimensional (2D) dip section of the margin displaying reservoir geometry and permeability distribution. Coupling our 2D permeability model with pore-water salinities allows an understanding of a revised distribution of the salinity at the margin scale, and the possible pathways and emplacement mechanisms for the fresh and salty water below the New Jersey shelf.

## GEOLOGICAL AND HYDROGEOLOGICAL BACKGROUNDS

The New Jersey Margin is a classic passive margin; continental rifting there began in the Late Triassic, and seafloor spreading was established by the Early to early-Middle Jurassic (Withjack and Schlische, 2005; Withjack et al., 2012). Subsequent tectonics have been dominated by thermal subsidence, sediment loading, and flexure (Watts and Steckler, 1979). The most recent deposits consist of Late Oligocene to Holocene siliciclastic clinoform wedges, as seen on offshore multichannel reflection seismic profiles acquired on the inner-middle shelf (Monteverde et al., 2000). During Expedition 313, three sites were drilled and cored 45–67 km offshore (Fig. 1A), at water depths of ~35 m, targeting the topsets, foresets, and bottomsets of several clinoforms (Mountain et al., 2010). As detailed in Mountain et al. (2010), the main sedimentary facies range from clay to sands that are locally cemented (by mineral precipitation) or lithified (through compaction and cementation). The cores reveal silt-rich supply systems notably depleted in clays (in terms of grain size) and show a marked difference in facies between topset beds landward of clinoform rollovers, and bottomset beds seaward of the clinoform toes (Proust et al., 2010). The topset facies consist of well-sorted silts and sands that were deposited in offshore to shoreface, mixed wave- to river-dominated shelf environments. The bottomset facies comprise silts and silty clays that were deposited below wave base, typically interbedded with poorly sorted silts and sands deposited by downslope gravity transport processes. Glauconite-rich horizons represent a common component of topset and bottomset strata. Several lithostratigraphic units have also been recognized and correlated across sites (Mountain et al., 2010). The results of Expedition 313 also benefit from established lithological and chronostratigraphic constraints on the depositional sequences provided by previous drilling: Ocean Drilling Program (ODP) Legs 150, 150X, 174, 174X and onshore International Continental Drilling Program boreholes (Miller et al., 1994; Mountain et al., 1994; Austin et al., 1998); the Atlantic Margin Coring Project (AMCOR) (Hathaway et al., 1976); and the Atlantic City Offshore Well Program (ACOW) (McAuley et al., 2001; Mullikin, 1990).

Beneath the New Jersey coastal plain, a multilayered system saturated with fresh water is developed in unconsolidated siliciclastic deposits of Miocene age (Barlow, 2003; Barton et al., 1993; Miller and Snyder, 1998; Szabo et al., 2006). Due to onshore pumping and salt-water intrusion, the upper unconfined aquifer (surficial Kirkwood-Cohansey) commonly contains brackish or salty water at the coastline. Offshore, the presence of pore water fresher than seawater is known from a series of boreholes completed along the Atlantic continental shelf during the 1970s and 1980s as part of AMCOR (Hathaway et al., 1976), the Continental Offshore Stratigraphic Test (Schlee and Fritsch, 1982), ACOW (McAuley et al., 2001), and ODP Legs 150 and 174A wells (Austin et al., 1998; Malone et al., 2002; Mountain et al., 1994) (Table 1). Chlorinity concentrations below that of seawater have thus been noted at least 130 km

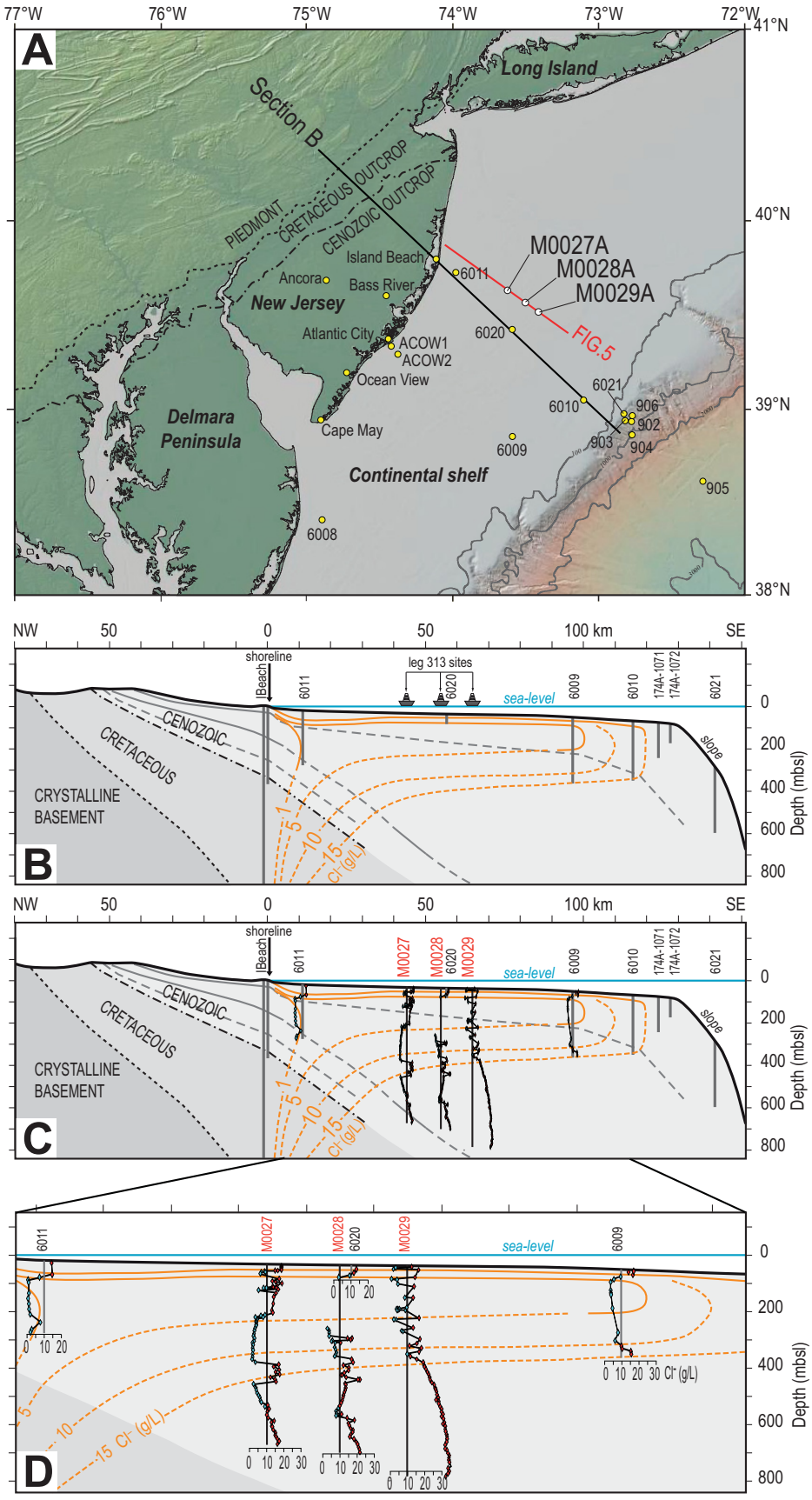


**Figure 1. (A) The New Jersey continental margin showing the locations of Integrated Ocean Drilling Program Expedition 313 Holes M0027A, M0028A, and M0029A, and previous onshore and offshore boreholes (from Mountain et al., 2010) (ACOW—Atlantic City Offshore Well Program). (B) Hydrogeological section of the New Jersey Margin classically used for groundwater-flow modeling (modified from Hathaway et al., 1979), showing the pore-water chlorinity distribution in the offshore domain. Dashed lines are extrapolations, and not based on field data (mbsl—meters below sea level). (C) As in B, but including the superimposed Expedition 313 chlorinity pore-water data (in g/L). Recent borehole data allow the original model to be refined. The pore-water units are numerous, with a multilayered organization at the three sites drilled. Several intervals of fresher water (in blue; chlorinity < 10 g/L) alternate with saltier intervals (in red; chlorinity > 10 g/L). Seawater chlorinity is typically ~19 g/L. (D) Enlarged view of the middle shelf area.**

offshore. This fresh to brackish fluid is interpreted by some as being relict Pleistocene water (Hathaway et al., 1979; Kohout et al., 1988). Geochemical analysis of interstitial waters of Expedition 313 (van Geldern et al., 2013) shows that the fresh-water stable isotope ratios are identical to those of modern precipitation in New Jersey. This indicates either a modern age, or that the water was recharged at a time with climatic and hydrologic conditions similar to modern conditions (van Geldern et al., 2013). No absolute ages are available from Expedition 313 to help distinguish between these possibilities. Based on a transect of five holes across the shelf, Hathaway et al. (1979) proposed a hydrogeologic conceptual model for the offshore New Jersey (Fig. 1B) with a thick subhorizontal lens of relatively fresh groundwater (minimum chlorinity < 1 g/L) at ~150 mbsf and extending from the coastline (AMCOR sites 6008 and 6011) to more than 100 km offshore (AMCOR site 6009). Overlying this lens is an extremely sharp chlorinity gradient, increasing upward to approach the chlorinity of seawater (AMCOR sites 6008, 6011, 6009). Hathaway et al. (1979) noted that this gradient occurs in low-permeability clay acting as a confining unit for the underlying permeable beds of the Kirkwood Formation (which were under artesian pressure prior to intensive groundwater development). Hathaway et al. (1979) suggested that the presence of this confining bed has been an impediment to rapid

TABLE 1. COMPILATION OF EXISTING PORE WATER CHLORINITY IN THE BOREHOLES DRILLED ON THE NEW JERSEY MARGIN

| IODP Expedition or Drilling Program | Site | Water depth (m) | Maximum penetration (mbsf) | Distance from shore (km) | Minimum chloride concentration (mM)† | Depth of minimum chloride concentration (mbsf) | Maximum chloride concentration (mM)† | Depth of maximum chloride concentration (mbsf) | References |
|---|---|---|---|---|---|---|---|---|---|
| ODP Leg 174A | 1071 | 88 | 424.2 | 129 | 426 | 49.79 | 576 | 369.48 | Austin et al., 1998 |
| ODP Leg 174A | 1072 | 98 | 358.6 | 127 | 469 | 63.9 | 569 | 230.5 | Austin et al., 1998 |
| ODP Leg 174A | 1073 | 639 | 663.6 | 169 | 554 | 72.5 | 582 | 641.65 | Austin et al., 1998 |
| ODP Leg 150 | 902 | 808 | 740.1 | 144 | 546 | 35.97 | 962 | 692.8 | Mountain et al., 1994 |
| ODP Leg 150 | 903 | 446.4 | 1149.7 | 142 | 556 | 196.35 | 986 | 1089.3 | Mountain et al., 1994 |
| ODP Leg 150 | 904 | 1122.8 | 576.7 | 150 | 565 | 4.4 | 951 | 558.7 | Mountain et al., 1994 |
| ODP Leg 150 | 905 | 2697.9 | 910.6 | 200 | 522 | 823.1 | 558 | 21.45 | Mountain et al., 1994 |
| ODP Leg 150 | 906 | 912.9 | 602.4 | 145 | 563 | 1.45 | 992 | 509.1 | Mountain et al., 1994 |
| AMCOR | 6008 | 20.7 | 119.5 | 15 | 5.6 | 59.3 | | | Hathaway et al., 1979 |
| AMCOR | 6009 | 58.5 | 299.6 | 90 | 90.3 | 79.5 | | | Hathaway et al., 1979 |
| AMCOR | 6010 | 75.9 | 310.6 | 100 | 372.4 | 216.1 | | | Hathaway et al., 1979 |
| AMCOR | 6011 | 22.3 | 260 | 12 | 22.6 | 70.7 | | | Hathaway et al., 1979 |
| AMCOR | 6020 | 39 | 43.9 | 56 | 112.8 | 44 | | | Hathaway et al., 1979 |
| AMCOR | 6021 | 301.2 | 304.8 | 140 | 527.5 | 3.8 | | | Hathaway et al., 1979 |
| Leg 313 | M0027A | 33.53 | 631.01 | 43 | 40.8 | 330.54 | 529 | 62.29 | Mountain et al., 2010; this study |
| Leg 313 | M0028A* | 35.05 | 668.66 | 56 | 72.3 | 224.81 | 607.6 | 663.67 | Mountain et al., 2010; this study |
| Leg 313 | M0029A | 35.97 | 754.55 | 67 | 19.5 | 49.98 | 994.5 | 711 | Mountain et al., 2010; this study |

*Note:* IODP—Integrated Ocean Drilling Program; ODP—Ocean Drilling Program; AMCOR—Atlantic Margin Coring Project; mbsf—meters below seafloor.
*Uppermost 224 m not cored at this site.
†Standard seawater chloride concentration: 559 mM.

downward seawater infiltration and penetration in onshore fresh-water aquifers. The outer shelf and upper slope drill sites (ODP Legs 150 and 174A; Table 1) show no or only slight decrease in pore-water chlorinity with depth, with values close to that of seawater (~524 mM, ~19 g/L). Positive anomalies in pore-water salinity (to 40 g/L) have also been observed locally beneath the shelf, especially off Florida (e.g., AMCOR site 6002). These high salinities are attributed to upward diffusion processes related to deeply buried evaporite deposits (Manheim and Paull, 1981; Toth and Lerman, 1975).

The presence of fresh or brackish water on the New Jersey Margin was already known prior to Expedition 313. However, most interstitial water studies on this shelf were limited to the uppermost hundred meters of the sediment column, and to the nearshore or outer shelf regions. This is principally due to the considerable difficulties of drilling in shallow waters and non-consolidated sediments (e.g., the core recovery of the AMCOR 6011 Hole is only 26%). The existing boreholes were thus relatively shallow (Table 1) and not very numerous. Expedition 313 boreholes provide the first evidence for fresh water with salinities below 3 g/L as deep as 400 mbsf and as far as 45 km offshore (Mountain et al., 2010); this is significantly fresher than previously observed in this sector of the shelf (e.g., AMCOR site 6020) (Hathaway et al., 1976). These data are critical for refining our knowledge of the pore-water salinity distribution at depth, on a passive margin, in a place where information is scarce.

## DATA AND METHODS

### Expedition 313 Data

Expedition 313 drilled three 631–755-m-deep boreholes on the New Jersey middle shelf, gathering a full set of geophysical data tied to boreholes cored with 80% recovery. Expedition 313 (April–June 2009) measurements relevant to this work are briefly presented herein; they include downhole log data, petrophysical and pore-water geochemical measurements on full length cores, and core samples (for further details, see Mountain et al., 2010).

More than 5800 m of downhole logging data are available from Expedition 313, including spectral gamma-ray and sonic velocity measurements. The spectral gamma-ray data provide a measurement of the content of individual radioactive elements (potassium, uranium, and thorium) in the sediment, allowing the identification of the main sedimentary units (Serra, 1984). Statistical analysis performed on these data allows a prediction of lithologies (Inwood

et al., 2010, 2013). The sonic data provide the compressional wave velocity (Vp) of the formation, with velocity peaks observed in cemented horizons (Mountain et al., 2010).

Bulk density and velocity measurements were acquired on whole cores during the expedition using a Geotek multisensor core logger (www.geotek.co.uk). Moisture and bulk density measurements were performed at the Bremen core repository on discrete samples taken from the split cores with a vertical sampling rate of one measurement per core (i.e., per 3 m). These measurements provide, among other values, derived total porosity (phi) (see methodology in Mountain et al., 2010). Additional porosity measurements (same method as described above) were done in the Montpellier University laboratory on 10 samples on which we also measured permeability (see Table 2 and following methodology description). Note that the porosity mentioned herein refers to the total porosity phi (including noninterconnected pore space and space filled by bound water), while in hydrogeological terms the porosity that contributes to fluid flow though the rock is termed effective porosity $phi_{eff}$. With this definition, clayey material has a high total porosity and a low effective porosity, while sand has a low total porosity and a high effective porosity; therefore, fluid flow is enhanced in sand and slow in clay.

Interstitial water sampling was performed offshore using Rhizon samplers or by squeezing whole round sections, with a vertical sampling rate of one measurement per three cores (i.e., every 9 m). Water samples were analyzed onboard for pH, alkalinity, ammonium, and salinity. Successive analyses provided the concentrations of major and minor ions, allowing the assessment of pore-water salinities (see Mountain et al., 2010, for more details). Several classification methods have been developed to differentiate between fresh water, brackish water, and salt water. Water with total dissolved solids (TDS) concentrations <1 g/L is usually referred to as fresh (Barlow, 2003). Such low concentrations are not observed in Expedition 313 pore waters and in this study; we refer to water as fresh when TDS concentration is <15 g/L. In some places the measured concentrations are lower than this threshold, but this arbitrary upper limit has been chosen to facilitate discussion. In the following text, we use the term salinity to refer to TDS concentrations.

## Gas Permeability Measurements

We sampled 10 mini core plugs (diameter 9 mm, length 20 mm) for petrophysical studies (Table 2). Gas permeability measurements on these plugs were done under steady-state conditions using standard engineering methods with differential pressure transducers and mass flow meters (Bloomfield and Williams, 1995). An isotropic confined pressure of 100 bar was applied to the sample. Argon gas was injected into the core plug at a constant pressure, while the downstream end of the sample remained at atmospheric pressure. Differential pressures applied ranged from $0.2 \times 10^5$ Pa to $15 \times 10^5$ Pa, and flow rates ranged from $5 \times 10^{-5}$ L/min to 0.3 L/min. These permeability measurements have a relative precision of at least 5%. The measured permeabilities ($k$) were corrected for the Klinkenberg gas slippage effect as necessary (Klinkenberg, 1941; Tanikawa and Shimamoto, 2006). Due to the sampling method (plugs are oriented perpendicular to the core slab), we measured the horizontal permeability (i.e., permeability parallel to the sedimentary beddings). Permeability measurements have not been performed on nonconsolidated samples.

## Seismic Profiles and Facies Analysis

Seismic lines from two separate cruises (Oc270 [R/V *Oceanus* cruise 270] and CH0698 [R/V *Cape Hatteras* cruise 0698]) were used in this study to construct a dip line for 2D seismic facies and lithofacies analysis. Seismic data collected in 1995 on Oc270 dominantly sampled the outer New Jersey continental margin. From this survey, the dip-oriented line 529 has been used to image the proposed sites for the Expedition 313 holes. In 1998, seismic data acquisition on CH0698 sampled the inner coastal regional with line 19 intersecting line 529 (Oc270) and continuing the margin dip profile as close to shore as possible (Fig. 1). These two seismic lines combine to form a dip profile that intersects Expedition 313 holes with sufficient resolution to allow detailed facies analysis. Oc270 and CH0698 have similar seismic acquisitions, comprising a 48-channel, 600 m streamer towed at 2 or 4 m depths (depending on sea state). The data were recorded with an OYO DAS-1 seismograph with trace lengths of 2 s and sample rates of 1 ms on Oc270 and 0.5 ms on CH0698. Data imaging nears a vertical resolution of 5 m with sufficient clarity down to ~1.3 s of two-way traveltime (TWT) before resolution breaks down. Seafloor multiples have been sufficiently suppressed, though peg-leg multiples still remain, generally below more steeply dipping reflectors. (For details on seismic acquisition and processing, see Monteverde, 2008.)

Detailed visual descriptions of the lithofacies were performed on split cores (Mountain et al., 2010) and complemented by grain size analysis of 1700 samples (J.V. Browning et al., 2013, personal commun.). The lithofacies were interpreted in terms of depositional environments and their stacking patterns were interpreted in terms of systems tracts and depositional sequences (J.N. Proust, 2013, personal commun.). The lithofacies succession in the three holes was tied to the downhole gamma-ray logs (Inwood et al., 2013). Wireline sonic logs acquired in the holes and calculation of synthetic seismograms from the multisensor core logger data tie the lithofacies description to the on-site seismic line 529 (Oc270) (Miller et al., 2013a). The accurate ties at the three holes between the seismic data, the lithologies, the depositional environments, and sequences led to the construction of a 2D cross section of the margin along seismic lines 19 and

TABLE 2. TOTAL POROSITY AND PERMEABILITY MEASUREMENTS ON CORE SAMPLES TAKEN FROM CEMENTED HORIZONS OBSERVED AT OR CLOSE TO THE TRANSITION BETWEEN FRESH PORE WATER AND SALT PORE WATER UNITS

| Sample number | Site | Core | Sample depth (mcsf) | Lithology | Onshore party porosity (%) | Laboratory porosity (%) | Laboratory permeability $k$ (mD) |
|---|---|---|---|---|---|---|---|
| P1 | M0027A | 171-R1 | 489.77 | glauconitic sandstones | 37.6 | 46.3 | 75 |
| P2 | M0027A | 174-R1 | 494.51 | glauconitic sandstones | 34.5 | 40.1 | 43 |
| P3 | M0027A | 174-R1 | 494.51 | glauconitic sandstones | 34.5 | 45.7 | 6 |
| P4 | M0028A | 12-R1 | 254.01 | brown silty claystone | 56.3 | 53.0 | 0.1 |
| P5 | M0028A | 40-R1 | 327.55 | glauconitic sandstone | 46.6 | 31.8 | 2.5 |
| P6 | M0028A | 123-R1 | 540.04 | glauconitic sandstone | 7 | 24.0 | 0.008 |
| P7 | M0029A | 72-R1 | 343.58 | gray siltstone | — | 3.0 | 0.0006 |
| P8 | M0029A | 119-R1 | 479.52 | gray siltstone | — | 0.4 | $<10^{-4}$ |
| P9 | M0029A | 164-R2 | 611.87 | gray sandstone | — | 14.0 | 0.004 |
| P10 | M0029A | 173-R1 | 636.23 | glauconitic sandstone | 28.2 | 29.1 | 0.4 |

*Note:* See Figures 2 and 4 for sample location in the boreholes; mcsf—core depth below sea floor; dash—no measurement performed at this depth.

529. This cross section shows the lateral distribution of the lithofacies and systems tracts (J.N. Proust, 2013, personal commun.) and has subsequently been interpreted in terms of 2D reservoir geometry and permeability distribution.

### 2D Reservoir Geometry along a Dip Section and Permeability Distribution

We present a 2D dip section of the margin, displaying reservoir geometry and permeability distribution, inferred by combining clinoform geometries, system tracts, and seismic facies distribution. Lithofacies and predicted sedimentary facies have also been taken into consideration based on the work of J.N. Proust (2013, personal commun.), who tied a series of sedimentary facies and depositional environments from Expedition 313 core analyses to seismic profiles. We have interpreted these sedimentary facies in terms of expected permeability ranges (Bear, 1971), and regrouped them under three classes of permeability. (1) Permeable deposits ($k$ estimated to be $>10^3$ mD [1 mD = $10^{-15}$ m$^2$]) group nonconsolidated coarse-grained–dominated sediments that accumulated in foreshore, shoreface, and shoreface transitional environments. Bypass gullies and channel-fill deposits are also expected to belong to this category. (2) Semipermeable deposits ($1 < k < 10^3$ mD) accumulated in slope apron and toe-of-slope apron depositional environments. Although mainly coarse grained, these sediments recovered at depth have been affected by compaction processes, so their initial porosity (and inferred permeability) has been reduced. (3) Low-permeability deposits ($k < 1$ mD) group predominantly fine-grained sediments (silts and clays) that accumulated offshore (below fair weather wave base).

In the upper part of the Expedition 313 drill sites, where few or no cores have been taken, we used the lithologies predicted from downhole logging data statistical analysis (Inwood et al., 2013). Close to the coast, we used the downhole gamma-ray logs from ODP Leg 150X Island Beach and AMCOR 2011 holes (Hathaway et al., 1976; Miller et al., 1994) to refine the permeability distribution. These logs have been converted from depth (m) to time (TWT) (Monteverde, 2008) and subsequently projected onto CH0698 line 19. Despite some uncertainties resulting from this projection and associated possible lateral sedimentological variations, these logs allowed coarse-grained intervals (low gamma-ray values in the absence of glauconite) to be distinguished from fine-grained intervals (high gamma-ray values) beneath the inner shelf. Sandy intervals have been considered as permeable ($k > 10^3$ mD).

### Vertical Diffusion Time Estimates

An estimate of vertical diffusion times (for $Cl^-$ ions) has been performed for the permeable units ($k > 10^3$ mD) and low-permeability units ($k < 1$ mD) at the drill sites. The diffusion time $t_{diff}$ is given by $t_{diff} = L^2/D$, where D is the diffusion coefficient (of a dissolved species in sediment) in a porous medium, and L is the unit thickness. According to Berner (1980), $D = D_0/\tau^2$, where $D_0$ is the molecular diffusion coefficient in pore water (in the absence of sediment particles) and $\tau^2$ is the tortuosity. The tortuosity is given by $\tau^2 = phi_{eff} \cdot F$ where phi is the porosity and F is the formation factor and is given by $F \approx phi_{eff}^{(-m)}$ (Archie, 1942), and m is the cementation exponent. We assigned a value of m = 1.5 in the nonconsolidated permeable sands and m = 3 in the nonconsolidated low-permeability silty clays (Revil and Cathles, 1999). $D_0$ for most common ions is in the range $1 \times 10^{-9}$ to $2 \times 10^{-9}$ m$^2$ s$^{-1}$. We used $D_0 = 1.7 \times 10^{-9}$ m$^2$ s$^{-1}$ for $Cl^-$ ions (Li and Gregory, 1974). For a given sedimentary unit, the mean total porosity across the unit has been used. The parameters used and calculations are presented in Table 3.

## RESULTS

### Hole M0027A

Hole M0027A is the most proximal site drilled in the shallow shelf during Expedition 313. It is located 43 km offshore, in a water depth of 34 m. The hole reached 631 mbsf, and passed through deposits ranging from Late Eocene to Pleistocene in age (Mountain et al., 2010).

Geochemical analyses of pore waters (Mountain et al., 2010; van Geldern et al., 2013) show a wide range of salinities (2.6–34 g/L). As shown in Figure 2A, the vertical changes in salinities reveal the presence of a multilayered system. Intervals saturated with relatively fresh water (salinity < 15 g/L) alternate with others saturated with relatively salty water (salinity > 15 g/L), often close to the salinity of seawater (~35 g/L). Several pore-water units can thus be distinguished. Transitions between two successive units are often sharp. For example, at ~350 and ~412 mbsf, salinity passes from >25 to <5 g/L over a 10-m-thick interval. The thickness of the pore-water units is variable, reaching 170 m in a fresh-water interval between 180–350 mbsf (Fig. 2A). Units can also be as thin as 10 m (e.g., 70–80 mbsf) or few tens of meters (e.g., 15–40 mbsf).

The distribution of the fresh water–salt water varies closely with the lithology (Fig. 2A). Fresher pore waters correlate with fine-grained intervals (e.g., 180–350 mbsf) and saltier pore waters correlate with coarse-grained intervals (e.g., 350–412 mbsf). This correlation is confirmed when plotting pore-water salinity against thorium (Th) content, and against total porosity (phi) (Fig. 3). The Th content in the sediment is a shale proxy, where high Th concentrations mostly reflect nondiagenetic clays (Ellis and Singer, 2007). Clayey material has a high total porosity (typically 40%–70%), while silt and sand have a lower total porosity (35%–50% and 20%–50%, respectively) (e.g., Sanders, 1998). Figure 3A shows inverse linear correlations, confirming that fresher water is stored in clayey intervals (high Th content and high total porosity) and saltier water in sandy intervals (low Th content and low total porosity).

The above relationship, observed at the scale of the hole, is also apparent at a smaller scale. Clear changes in salinity also occur across specific boundaries. For example, the salinity of the pore water at the transition between unit VIB and unit VIIA (490 mbsf, Fig. 4A) passes from fresher above (~10 g/L) to saltier below (15–20 g/L). This transition correlates with a change from dominantly silty sands (more porous) to sands and glauconite sands (less porous), and is thus lithology dependent, as supported by the plots of salinity against Th or phi (Fig. 4).

Centimeter- to decimeter-thick cemented horizons are frequently observed at the transition between two successive pore-water units (pink highlighted bands in Fig. 2). For example, such horizons are observed from ~489 to ~495 mbsf (Fig. 4A). They correspond to glauconitic siltstones and sandstones (cores 171R1–174R3), with a characteristic petrophysical signature: low phi, high density, and high Vp. Their glauconitic component is attested by low Th/K ratios. The permeability ($k$) of these two horizons has been measured in the laboratory on two samples taken at 494.51 mbsf that yielded permeabilities of 6 and 43 mD (P2 and P3, Table 2), consistent with values commonly observed in sandstones (Bear, 1971).

### Hole M0028A

Hole M0028A is the intermediate site drilled in the shallow shelf, 56 km offshore, in a water depth of 35 m. The hole reached 669 mbsf, and deposits range from Early to Middle Miocene (Mountain et al., 2010). The upper part of the sedimentary column (0–224 mbsf) has not been recovered at this site, but lithology can be indirectly assessed from statistical analysis performed on gamma-ray logs (Inwood et al., 2010; Inwood et al., 2013, personal commun.).

Geochemical analysis performed on pore waters reveals a configuration close to the one observed in M0027A with salinities ranging

TABLE 3. PROPERTIES OF THE MAIN RESERVOIRS (R2, R3, R4) AND LOW-PERMEABILITY UNITS (C2, C3, C4) AT THE IODP EXPEDITION 313 DRILL SITES

| | Site | Depth range (mbsf) | Thickness (m) | Dominant lithology | Other characteristics | Porosity range phi (%) | Mean porosity (%) | Pore-water salinity range TDS (g/L) | Mean pore water salinity TDS (g/L) | Permeability $k$ (mD) | Cementation exponent m | Tortuosity $\tau^2$ | Cl-molecular diffusion coefficient $D_0$ ($m^2/s$) | Diffusion coefficient D ($m^2/s$) | Vertical diffusion time $t_{diff}$ (s) | Vertical diffusion time $t_{diff}$ (m.y.) |
|---|---|---|---|---|---|---|---|---|---|---|---|---|---|---|---|---|
| MAIN RESERVOIRS | | | | | | | | | | | | | | | | |
| | M0027A | 0–172 | 172 | nonconsolidated sands | contains freshwater lenses in fine-grained horizons | 23–49 | 37.1 | 9–34 | 25.5 | >$10^3$ | 1.5 | 1.64 | 1.7E-09 | 1.0E-09 | 2.9E+13 | 0.91 |
| R4 | M0028A | 0–214 (not sampled) | 214 | nonconsolidated sands | contains freshwater lenses in fine-grained horizons | — | — | — | — | >$10^3$ | 1.5 | — | — | — | — | — |
| | M0029A | 0–312 | 312 | nonconsolidated sands | contains freshwater lenses in fine-grained horizons | 27–77 | 45.0 | 1.3–32.8 | 16 | >$10^3$ | 1.5 | 1.49 | 1.7E-09 | 1.1E-09 | 8.5E+13 | 2.71 |
| R3 | M0028A | 254–290 | 36 | nonconsolidated coarse sands | presence of cemented horizon in the lowermost part | 26–53 | 37.8 | 8.1–30.8 | 18.9 | >$10^3$ | 1.5 | 1.63 | 1.7E-09 | 1.0E-09 | 1.2E+12 | 0.04 |
| | M0028A | 329–448 | 175 | nonconsolidated coarse sands | bounded above by cemented horizons | 34–49 | 42.0 | 17.8–39.4 | 25.5 | >$10^3$ | 1.5 | 1.54 | 1.7E-09 | 1.1E-09 | 2.8E+13 | 0.88 |
| R2 | M0027A | 345–414 | 69 | nonconsolidated coarse sands | presence of cemented horizon in the lowermost part | 26–44 | 37.5 | 5.6–32 | 25.5 | >$10^3$ | 1.5 | 1.63 | 1.7E-09 | 1.0E-09 | 4.6E+12 | 0.15 |
| MAIN LOW PERMEABILITY INTERVALS | | | | | | | | | | | | | | | | |
| C4 | M0029A | 312–342 | 30 | nonconsolidated silts and clays | bounded below by cemented horizons | 43–41 | 47 | 17.3–27.2 | 21.8 | <1 | 3 | 4.53 | 1.7E-09 | 3.8E-10 | 2.4E+12 | 0.08 |
| C4 | M0029A | 336–459 | 123 | clay, silt, fine sand, glauconite rich | under brine influence | 41–54 | 48 | 32–45 | 38.3 | <1 | 3 | 4.34 | 1.7E-09 | 3.9E-10 | 3.9E+13 | 1.22 |
| C3 | M0027A | 172–345 | 173 | nonconsolidated silts and clays | bounded above by a cemented horizon | 31–62 | 48.6 | 2.6–15.7 | 5.9 | <1 | 3 | 4.23 | 1.7E-09 | 4.0E-10 | 7.5E+13 | 2.36 |
| C3c | M0028A | 214–254 | 40 | nonconsolidated clays | — | 49–57 | 52 | 5–6.5 | 5.9 | <1 | 3 | 3.70 | 1.7E-09 | 4.6E-10 | 3.5E+12 | 0.11 |
| C3b | M0028A | 290–329 | 39 | nonconsolidated silts and clays | bounded below by a cemented horizon | 48–58 | 53 | 11.4–13 | 12.1 | <1 | 3 | 3.56 | 1.7E-09 | 4.8E-10 | 3.2E+12 | 0.10 |
| C3b | M0029A | 506–602 | 96 | clay, silt, fine sand, glauconite rich | under brine influence, bounded below by cemented horizons | 45–61 | 51 | 48.9–57 | 50.9 | <1 | 3 | 3.84 | 1.7E-09 | 4.4E-10 | 2.1E+13 | 0.66 |
| C3a | M0028A | 448–528 | 80 | clay, silt, fine sand, glauconite rich | bounded below by cemented horizons | 39–53 | 47.8 | 12.6–20.3 | 16.8 | <1 | 3 | 4.38 | 1.7E-09 | 3.9E-10 | 1.6E+13 | 0.52 |
| C2 | M0027A | 414–488 | 74 | clay, silt, fine sand, glauconite rich | bounded below by cemented horizons | 36–55 | 46.5 | 3.8–11.3 | 8.1 | <1 | 3 | 4.62 | 1.7E-09 | 3.7E-10 | 1.5E+13 | 0.47 |
| C2 | M0028A | 612–661 | 49 | silty clays | under brine influence | 35–58 | 44.9 | 29.8–34.6 | 32.5 | <1 | 3 | 4.96 | 1.7E-09 | 3.4E-10 | 7.0E+12 | 0.22 |

*Note:* IODP—Integrated Ocean Drilling Program; mbsf—meters below seafloor; TDS—total dissolved solids; dash—no measurement performed at this depth.

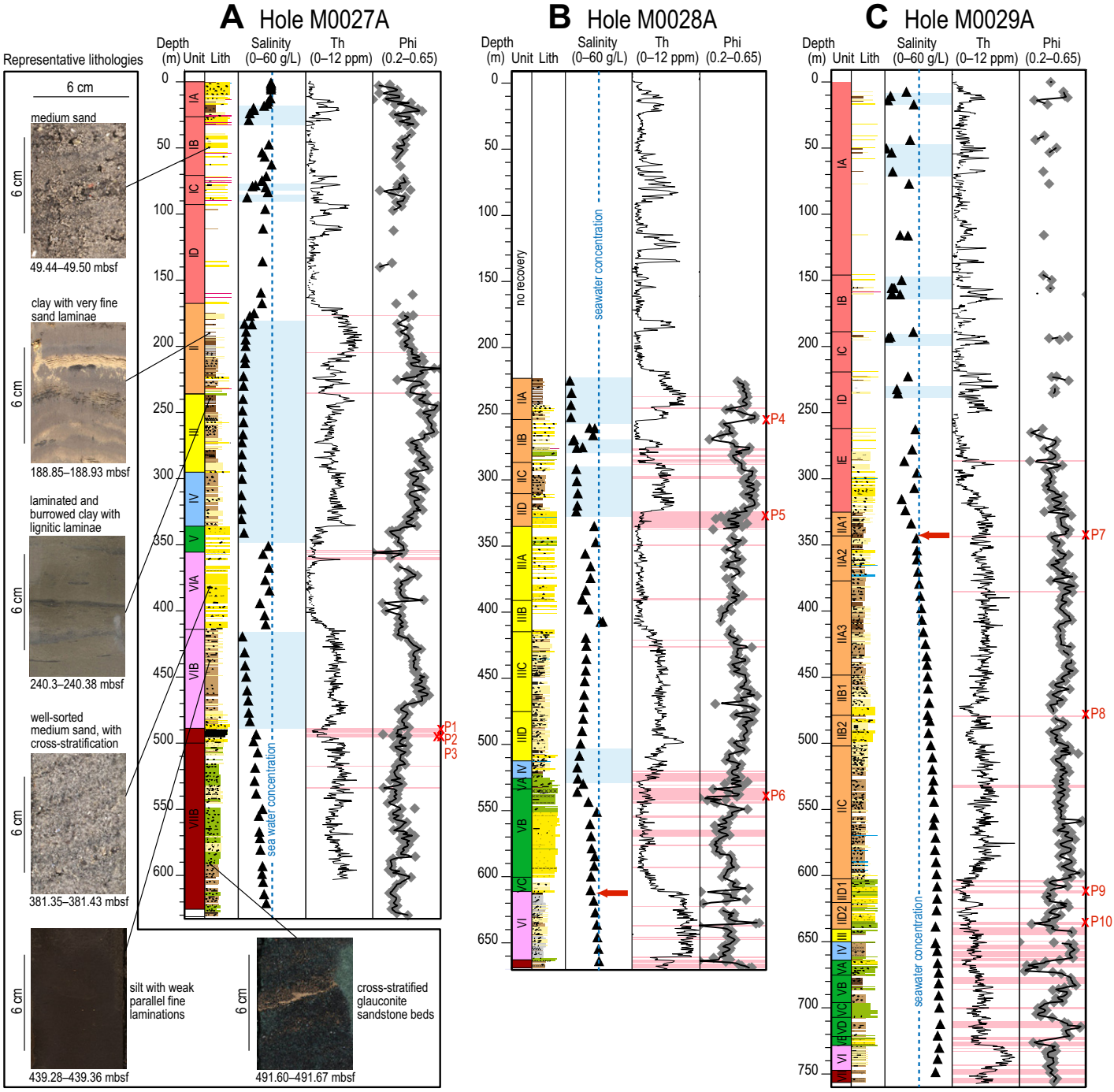


**Figure 2. Lithology (Lith), pore-water salinity, thorium content (Th), and porosity (phi) logs for Integrated Ocean Drilling Program Expedition 313 Holes M0027A, M0028A, and M0029A. Blue shading indicates fresh-water intervals (arbitrarily fixed threshold: total dissolved solids concentration < 15 g/L). Indurated or cemented intervals are indicated by pink shading. Red x symbols show the locations of permeability samples (see Table 2). Selected images of representative lithologies downhole are included on the far left (mbsf—meters below seafloor). Red arrows indicate depths at which pore-water salinity changes from a relatively linear correlation with lithology (above) to a scattered relationship (below) (see Fig. 3 and text).**

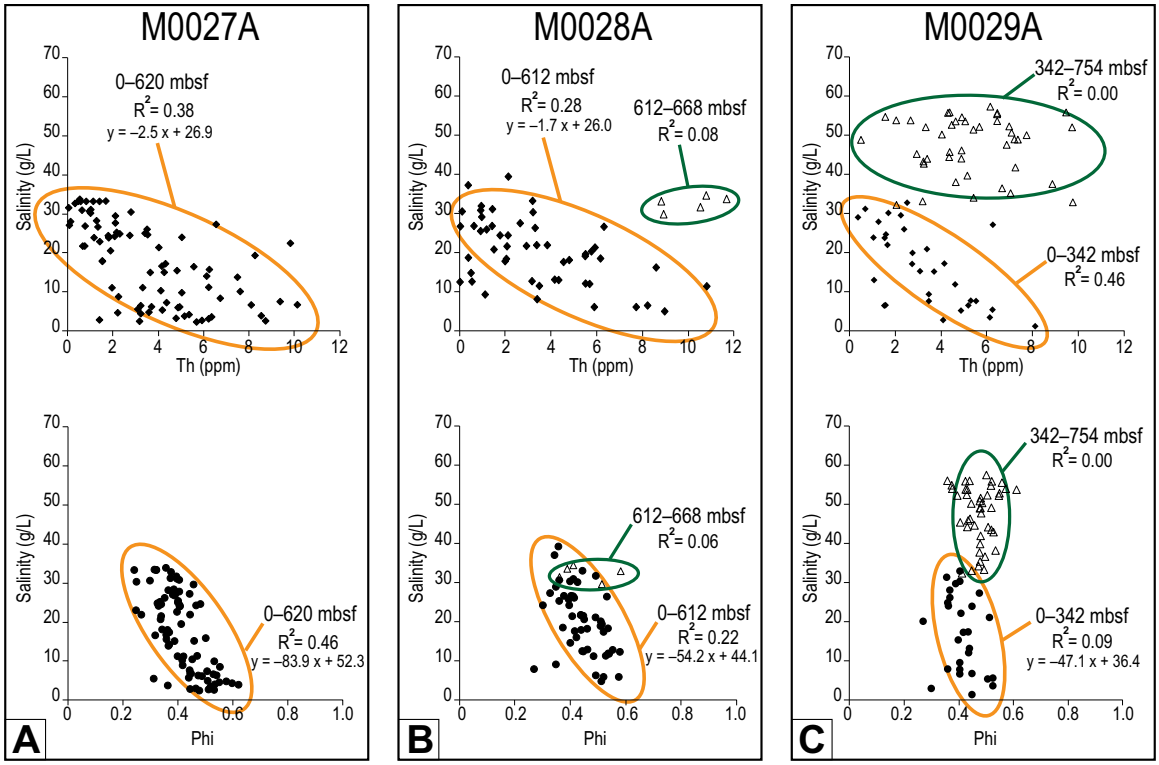


**Figure 3. Plots showing the relationship between pore-water salinity and Th (upper row) and pore-water salinity and porosity (phi) (lower row) for each hole of Integrated Ocean Drilling Program Expedition 313 (mbsf—meters below seafloor). R squared values are provided (the square of the Pearson product moment correlation coefficient). Equations for the best-fit line are given where R squared values indicate a linear correlation. From these plots it is clear that there is an inverse correlation between salinity with either Th or phi (data grouped within orange ovals, with R squared generally >0.20), reflecting the fact that saltier pore waters occur preferentially in coarse-grained intervals, whereas fresher pore waters occur in fine-grained intervals (see text). Deeper than 612 m in M0028A and 342 m in M0029A, the relationships differ from this inverse trend (data grouped within green ovals, with R squared close to zero) reflecting the presence of a pore-water unit under brine influence (see text).**

from 5 to 39.4 g/L (Mountain et al., 2010). Pore-water units are similarly organized into a multilayered system, though the fresh-water layers are slightly thinner and the stratifications appear to be slightly more irregular (Fig. 2B). Plots of the pore-water salinities (g/L) against phi or Th content show inverse linear correlations, illustrating that the salinity is lithology dependent, with fresher waters recovered in fine-grained intervals. This relationship does not apply to the lowermost part of the borehole (below 612 mbsf), where salty waters are observed in clay rich (high Th) intervals (Fig. 3B).

As observed in Hole M0027A, the transition between successive pore-water units is generally sharp, and locally correlates with cemented intervals. For example, the lower part of unit IID at ~325 mbsf marks the transition from fresher pore water above (~12 g/L), in clays to fine sands, to saltier water below (>20 g/L), in coarse sands (Fig. 4B). A cemented interval extending from ~324 to ~332 mbsf encompasses this transition. The low permeability of this cemented interval (characterized by decreased phi and increased density and sonic velocity), is confirmed by permeability measurements ($k$ = ~4 mD on a glauconitic sandstone sample taken at 327.55 mbsf; Table 2).

### Hole M0029A

Hole M0029A is the most distal site drilled in the shallow shelf, 67 km offshore, in a water depth of 36 m. The hole reached 755 mbsf, mainly recovering deposits of Miocene age (Mountain et al., 2010). The upper part of the sedimentary column (0–280 mbsf) has been spot cored at this site.

Pore-water salinities range from 1.3 to 57.5 g/L (Mountain et al., 2010). As for M0027A and most of M0028A, the uppermost pore-water units (above 342 mbsf) are organized in a multilayered system (Fig. 2C). Unlike the other holes, M0029A shows an increasingly saline brine below 342 mbsf, with chloride concentration reaching 995 mM (i.e., almost twice the concentration in seawater) and a $Cl/SO_4$ ratio different from the shallower samples (Mountain et al., 2010). In this interval, the salinity is unaffected by lithology, as is evident from the presence of brines in both clays and sands (e.g., 520–600 and 600–640 mbsf, respectively). Below 600 mbsf, phi shows considerable variability but there is no relationship with salinity. These observations are confirmed by the plots of the pore-water salinities against Th content and phi, showing two distinct trends at the scale of the hole (Fig. 3C). Above 342 mbsf, we observe an inverse linear correlation, again illustrating that the fresher waters are preferentially stored in fine-grained intervals. Below 342 m no correlation is observed, illustrating that the salinity is no longer lithology dependent.

Figure 4C illustrates the presence of a well-cemented horizon at the top of the pore-water unit under brine influence (below 342 mbsf),

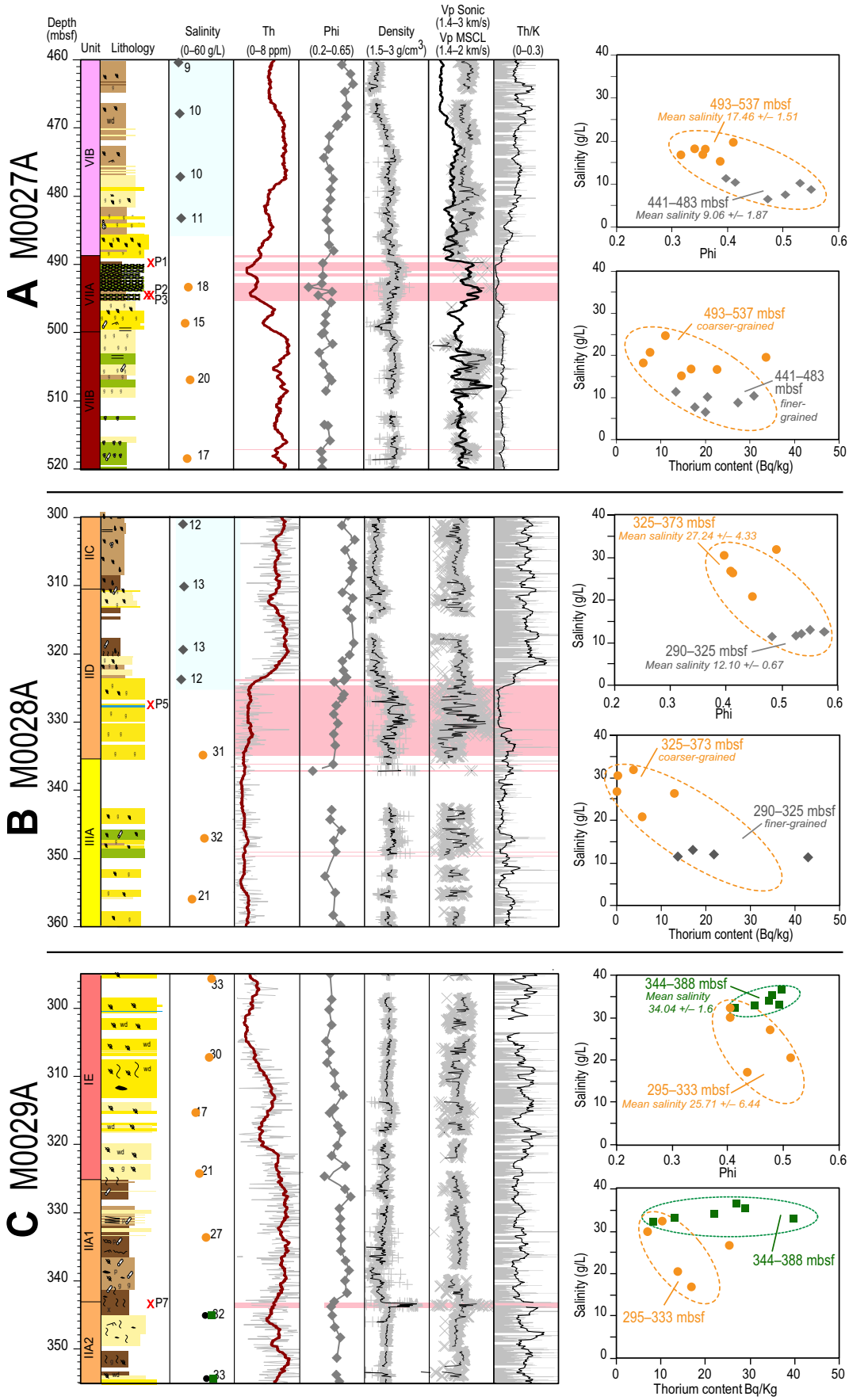


**Figure 4. (A–C) Selected intervals of low-permeability cemented horizons at salt water to fresh water transitions in Integrated Ocean Drilling Program Expedition 313 (mbsf—meters below seafloor) Holes M0027A, M0028A, and M0029A. Left: Pore-water salinity is given as total dissolved solids (TDS) concentration, Vp is compressional wave velocity (Full waveform sonic downhole probe and MSCL—multisensor core logger). Blue shading indicates fresh-water intervals (arbitrarily fixed threshold: TDS < 15 g/L). Indurated or cemented intervals are indicated by pink shading. Red x symbols indicate the location of permeability samples (see Table 2). Cemented horizons have a characteristic petrophysical signature (decreased porosity, increased density, and increased Vp). A low Th/K ratio reflects glauconite enrichment. Right: Plots showing the relationship between salinity and Th (upper row) and salinity and porosity (lower row) across each cemented horizon (mbsf—meters below seafloor). The mean and standard deviation of pore-water salinity are indicated on the upper plot in each borehole. In M0027A and M0028A, these plots illustrate an inverse correlation between salinity with either Th or phi (data grouped within orange ovals) across the cemented horizons. In M0029A, a clear departure from these linear correlations is observed below the cemented horizon (data grouped within green ovals), reflecting the presence of a pore-water unit under brine influence (see text).**

close to the transition between unit IIA2 and unit IIA1. A clear change in salinity trend is observed at this depth (Fig. 2C). An almost 1-m-thick cemented interval (343.3–343.8 mbsf, cores 71R2–72R1, gray siltstone) is especially well expressed in the petrophysical data by peaks in density (~2.65 g/cm$^3$) and sonic velocity (Fig. 4C). A sample taken from this interval at 343.58 m shows a low phi (3%) and a very low permeability ($k$ = ~6 × $10^{-4}$ mD) (Table 2). Another sample taken from a cemented layer ~50 m below this (479.52 mbsf), also in gray siltstones, yielded a phi of 0.4% and a permeability of <$10^{-4}$ mD, which is very low.

### Link Between Salinity, Seismic Facies, and Geometry of the Depositional Units at the Scale of the Margin

In the absence of deep upwelling brines, a strong correlation exists between fresh water–salt water distribution and lithology (Figs. 3 and 4), at least in the upper sections of the holes. Moreover, Figure 5A shows that there is a good correlation between pore-water salinities and seismic facies and clinoform morphology. This is especially clear for M0027A, where the uppermost 200-m-thick interval (i.e., shallower than ~0.3 s TWT), consisting of alternating salty and fresh pore-water units, correlates with a package of discontinuous seismic reflections. This characteristic seismic facies corresponds to the recent clinoform topsets that are sand dominated with locally interbedded clay layers (see also unit I in Fig. 2A). The underlying thick fresh-water interval mainly fits with another package of topsets, which are characterized by continuous high-amplitude reflections, gently dipping seaward, that are clay and silt dominated (units II, III, IV in Fig. 2A). The salty pore-water unit located below this thick fresh-water layer is in the vicinity of the rollover–inflection point, in the upper part of the clinoform foresets. These upper foresets are characterized by discontinuous to steeply dipping reflections, and consist of unconsolidated clean sand deposits (unit VIA in Fig. 2A). The lower part of the foresets is dominated by fine-grained deposits and is fresh-water bearing (unit VIB in Fig. 2A). The salinity increases downhole in M0027A in the bottomsets. Although less clear, similar features are observed in Hole M0028A, with fresh water stored in the fine-grained topsets and lower foresets, and salty water in the upper foresets. In Hole M0029A, this relationship is no longer true below ~0.4 s TWT (~342 mbsf), as it is overprinted by the presence of brines, and salinities have developed independent of the seismic facies.

## INTERPRETATION AND DISCUSSION

### Reservoir Geometry and Permeability Distribution at the Scale of the Margin

The present-day distribution of the salinity beneath the New Jersey shelf can be discussed in relation to the structure of the margin at several scales, from the lithology and/or permeability of the sediments at a small scale, to the geometry of the depositional units at the scale of the margin.

Based on the observations described in the preceding sections, we propose a 2D geometrical model along a dip section of the margin. This model shows the distribution of the reservoirs (defined here as high-permeability units with expected $k > 10^3$ mD) and low-permeability units ($k < 1$ mD), and their spatial heterogeneity. As shown in Figure 5B, the entire system consists of four main reservoirs, labeled R1 to R4, that are relatively disconnected. Reservoir R1, located close to the coastline, is made of sandy clinoform topsets and foresets deposits and contains fresh water. Reservoirs R2 and R3 contain salty water in a series of well-connected sandy upper foresets. Reservoir R4 is salty, with thin, elongated, low-permeability intervals containing fresh water; R4 is in the sandy topsets and is bounded above by a thin clayey unit possibly acting as a confining unit.

Reservoirs R2 to R4 were drilled during Expedition 313 (Figs. 2 and 5) and their characteristics in terms of salinity and porosity ranges are given in Table 3. Reservoirs R1 to R4 are separated from the others by low-permeability units of varied thicknesses and relatively broad spatial dimensions (blue in Fig. 5B). These units have been labeled C1 to C4. In terms of reservoir characterization, a geological unit is considered as permeable when $k > 1$ mD (Cossé, 1993), so these low-permeability units can still be considered as permeable. Their permeability is, however, expected to remain orders of magnitude lower than that of the nonconsolidated sands contained in reservoirs R2 to R4 (see Fig. 2; facies picture of unit VIA in Hole M0027A), and in which the permeability is expected to be >$10^3$ mD (Bear, 1971).

In the three holes of Expedition 313, cemented intervals often mark the salt water to fresh water transitions (pink shading in Figs. 2 and 4). They are especially noticeable at the top of R2 and R3, at the transition between the coarse-grained salty water-bearing foresets and the fine-grained fresh-water–bearing topsets (e.g., Hole M0027A, 360 mbsf; Hole M0028A, ~330 mbsf; Figs. 2 and 5B). The permeability $k$ measured in the cemented intervals yielded values below 10 mD, with the exception of two samples (Table 2), so the above cemented intervals can still be considered as permeable. For comparison, in unconsolidated clays, $k$ generally ranges from 10 to $10^{-2}$ mD (e.g., Revil and Cathles, 1999). Lower permeabilities ($k < 1$ mD) were measured in six samples, with two of these exhibiting very low values ($k < 10^{-3}$ mD) (samples P7 and P8, Table 2), suggesting that locally, such cemented horizons, if unfaulted, could form efficient permeability barriers. If active flows occur at the present time beneath the shelf, such horizons can strongly affect the flow path. Cemented horizons (and their lateral extrapolation) have been plotted in pink in Figure 5B at the fresh water–salt water boundaries.

### Revised Large-Scale Salinity Distribution

A series of analytical and paleohydrological and hydrological models was used to account for the distribution and origin of pore-water salinities beneath the New Jersey shelf, based on the hydrogeological conceptual model proposed by Hathaway et al. (1979) (Cohen et al., 2010; Kooi and Groen, 2000, 2001, 2003; Meisler et al., 1984). As shown in Figure 1B (modified from Hathaway et al., 1979), when penetrating vertically in the Cenozoic-aged deposits of the middle shelf, this model proposes a general groundwater pattern that consists of a sharp decrease in chlorinity with depth, from seawater concentration at the sea bed, down to a minimum concentration (<5 g/L) at ~150 mbsl. Below, the chlorinity increases downward (dashed lines) and reaches seawater concentrations at ~400 mbsf. Expedition 313 data allow the revision of this hydrogeological conceptual model.

In the shallowest levels of the model, the chlorinity gradient measured in the upper 50 m of M0027A is in good agreement with the one observed in AMCOR Hole 6020, drilled ~20 km away (Fig. 1C). This is not the case at Site M0029A, 20 km farther seaward, where low chloride concentrations were observed at shallower depths, from 10 to 13 mbsf. At greater depth, the salinity gradients measured during Expedition 313 in the Miocene series (see Mountain et al., 2010) contrast significantly with the existing model. For example, in M0027A, the chloride concentration of ~15 g/L at a depth of ~160 mbsf is greater than that predicted at the same depth (<5 g/L) (Fig. 1C). Conversely, at ~420 mbsf the measured chlorinities (<1.5 g/L) are 10 times lower than the predicted concentration (10–15 g/L). The observed pore-water units are also more numerous than predicted, with variable thicknesses, and a multilayered organization at the three sites drilled. In M0027A, at least five distinct intervals of fresh water of various thicknesses have

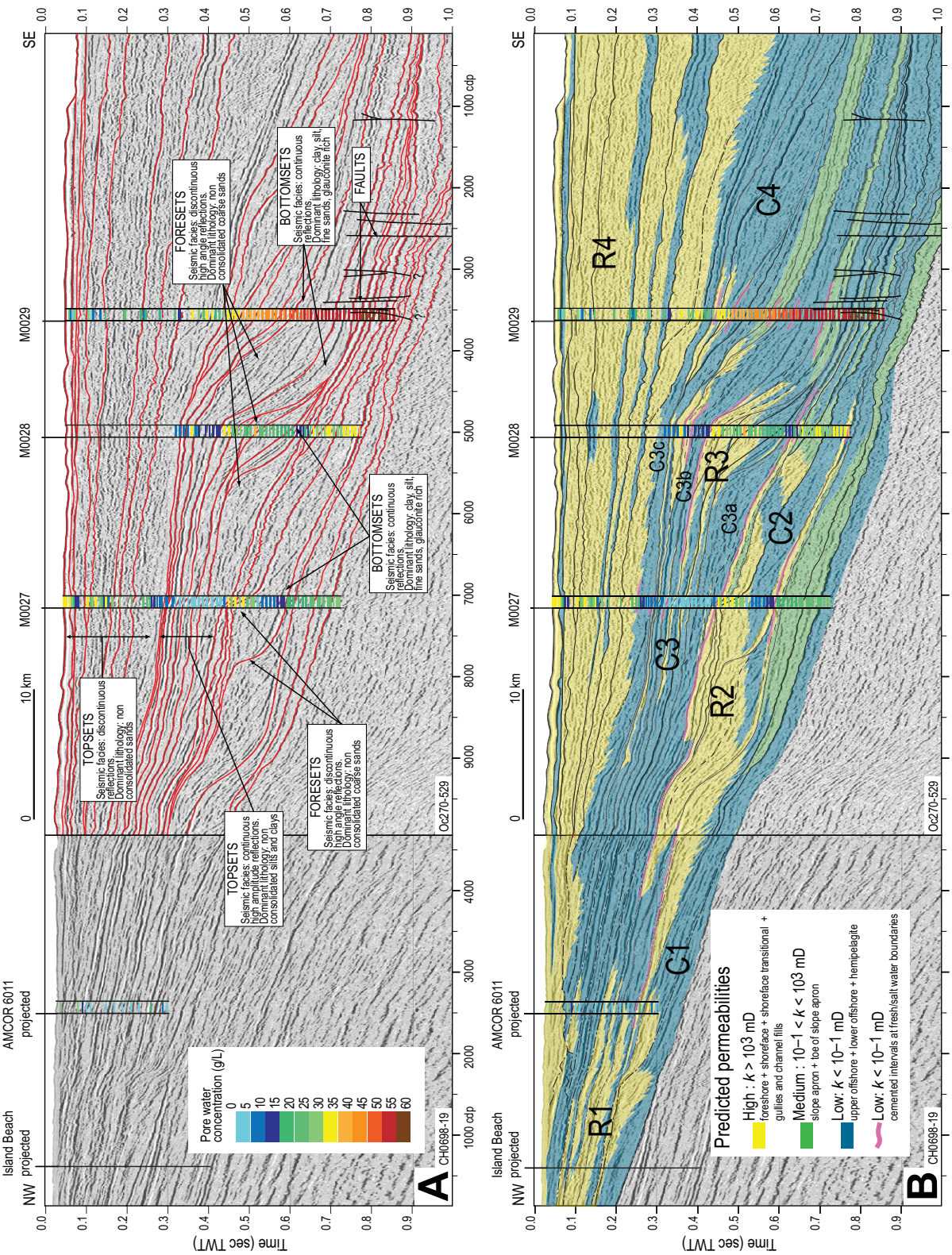


**Figure 5. Seismic lines Oc270–529 and CH0698–19 (R/V *Oceanus* cruise 270 and R/V *Cape Hatteras* cruise 0698) are combined to form a dip profile that intersects the Integrated Ocean Drilling Program Expedition 313 holes (location in Fig. 1), allowing both detailed facies analysis and larger scale geometry analysis (AMCOR—Atlantic Margin Coring Project; TWT—two-way traveltime; cdp–common depth point). Note reversed polarity on CH0698–19 as compared to Oc270–529. (A) Superimposed pore-water chlorinities from borehole data illustrate the clear correlation between seismic facies and salinity. (B) Two-dimensional reservoir model across the margin derived from combined clinoform geometries, systems tracts, seismic facies, and sedimentary facies analysis. The model illustrates the present-day architecture of the reservoirs (R1–R4; see text) and expected permeability (*k*) distribution. The main low-permeability units have been labeled C1–C3.**

been observed and four significantly freshened intervals in M0028A. Although, at this site, the upper sedimentary column was drilled with no core recovery, we anticipate that multiple fresh-water layers are similarly present, supported by a salinity of 5 g/L at 225 mbsf (the shallowest sample). A similar salinity pattern is observed in Hole M0029A where several layers of fresher water exist above 342 mbsf.

Another major difference with the conceptual model of Hathaway et al. (1979) is the location of the major fresh-water levels, and their relation to lithology. In the existing model, the thick fresh-water tongue ranges from ~100 to ~200 mbsf and is stored within coarse-grained deposits (shallow Miocene to Pleistocene sands) (Fig. 1B). On the contrary, Figure 1C shows that the thickest fresh-water intervals are much deeper, ranging from 190 to 350 mbsf in M0027A, and even deeper farther offshore, in M0028A. In M0027A, most of M0028A and the upper part of M0029A, fresh water is observed in fine-grained, clay-rich intervals (high total porosity, high Th), whereas salt water is mainly recovered in sands (low total porosity, low Th) (Fig. 3). This relationship is no longer true below 612 mbsf in M0028 and below 342 mbsf in M0029A, where the salinity varies independently of lithology (Fig. 3), suggesting that different mechanisms are involved in the emplacement of the pore-water salinity. This is consistent with the hypothesis that these intervals are dominated by advection-diffusion of deep rooted brines upwelling from depth (Mountain et al., 2010). Plots of pore-water chlorinity versus $\delta^{18}O$ values clearly illustrate a mixing line between brines and seawater below 340 mbsf in M0029A, and also suggest that the lower part of Hole M0027A (below 415 mbsf) is under the influence of brines (see fig. 10 in van Geldern et al., 2013). On seismic profiles, faults are observed close to Hole M0029A, in the lower part of the Miocene sequence (Fig. 5A). Such faults probably enhance upward brine migration originating from evaporites located at depth (Miller et al., 1994; van Geldern et al., 2013). The very low permeability cemented interval encountered at ~344 mbsf in Hole M0029A (sample P7, Fig. 2 and Table 2) is probably acting as an obstacle to upward advection of brines, as evidenced by the decreased salinity across this boundary, and the associated change in the salinity curve trend at this depth.

The differences between the conceptual model of Hathaway et al. (1979) with the one derived from Expedition 313 arise mainly from the pre-2009 absence of deep boreholes penetrating the middle shelf. Previous works were consequently based on extrapolated chlorinities between sites 6011 and 6009, with a distance of ~80 km (dotted lines in Fig. 1B). In addition, the pore-water sampling resolution during Expedition 313 (every ~10 m) was much higher and more regular than the one on the AMCOR boreholes (every 10–50 m), where the lower core recovery (often <30%, Hathaway et al., 1976) hindered sampling at higher resolution. These observations clearly illustrate that detailed sampling is of primary importance for the characterization of complex anisotropic geological environments such as prograding clastic margins. To assess groundwater flows, the spatial geological heterogeneity of these systems must be taken into consideration at several scales.

## Pathways and Possible Emplacement Mechanisms

Two main hypotheses might explain the presence of fresh water offshore on the New Jersey shelf. The first involves trapped meteoritic and/or sub–ice-sheet waters recharged during lowered sea-level periods (Cohen et al., 2010; Kooi and Groen, 2001; Person et al., 2003; Hathaway et al., 1979), while the second involves possible present-day active dynamic connections with onshore aquifers (van Geldern et al., 2013). Coupling our 2D permeability model with pore-water salinities facilitates discussion of the possible pathways and emplacement mechanisms for the fresh and salty water below the New Jersey shelf (excluding intervals affected by upwelling brines) and to tentatively test if the proposed hypotheses are compatible with the observed reservoir geometries.

McHugh et al. (2010) placed the Last Glacial Maximum (LGM) paleoshoreline at the 120 m isobath. During periods of lowered sea level (and during part of the subsequent transgressions) the Expedition 313 drilling sites were located a considerable distance landward (>50 km) of the shoreline. It is thus likely that both the high- and low-permeability units of the New Jersey shelf have been recharged with fresh water as a result of shelf exposure, meteoritic and/or sub–ice-sheet recharge, and elevated hydraulic gradient. Whether the pore waters beneath the shelf can still locally contain a record of previous low-stands, or alternatively, whether old hydrological events have been overprinted by the LGM phase, subsequent transgression, or by modern recharge remains a question. Currently, at the Expedition 313 drilling sites, fresh water is preferentially stored in fine-grained low-permeability units (C1–C3, Fig. 5B; mean salinities ranging from 5.9 to 16.8 g/L; Table 3), while salty water occurs in the coarse-grained deposits forming the permeable reservoirs (R2–R4, Fig. 5B; mean salinities ranging from 16 to 25.5 g/L; Table 3). Table 3 synthesizes the characteristics of R2–R4 and C2–C3, in terms of salinity and porosity at the drilling sites.

### *Fossil Water*

In the first hypothesis, the fresh water stored in C1–C4 and in the clay lenses contained in R4 (Fig. 5B) would be fossil (i.e., recharged during the LGM or possibly earlier). This implies that at the present time either these layers are not connected to onshore aquifers or onshore hydraulic heads are too low to drive modern meteoric water far offshore within these layers. This also implies that these fresh layers have not undergone salinization since the LGM. Diffusion time estimates within C2 and C3 at the drilling sites range from 0.1 to 2.36 m.y., supporting the idea that salinization of these layers by vertical diffusion over the past 0.02 m.y. is unlikely (Table 3). The petrophysical characteristics of the sediments (high total porosities and low permeabilities) allow them to hold a large volume of water, but prevent them from being rapidly flushed, and may have prevented seawater intrusion by density flow. The clay layers bearing fresh water in R4, as well as the clay layer at its top, are less than 20 m thick, and more often less than 10 m thick. Assuming a mean total porosity of 50%, the vertical diffusion times in these layers would range from 0.01 to 0.03 m.y., suggesting a possible salinization. However, this is in the uncertainty range of the calculation (e.g., assumption done on the cementation exponent m).

As shown in Table 3, the presence of salt water in the more permeable units (coarse-grained sands in reservoirs R2–R4; Fig. 5B) cannot be explained by vertical diffusion as the diffusion times within these reservoirs are too long (to 2.71 m.y. in R4). A rapid flushing of the LGM fresh water due to density-driven flow is proposed as the dominant solute transport mechanism, suggesting that reservoirs R2–R4 are currently connected with the sea. Such a connection can be either direct, via some strata of the reservoir cropping out on the seafloor, or indirect, via a series of intermediary connected reservoirs. The shallowest and the thickest reservoir, R4 (>300 m in M0029A; Table 3), located in coarse-grained topsets, thickens seaward and thins landward, almost disappearing at the coastline (Fig. 5B). This 2D geometry suggests that R4 is not connected to the land at the present time and is not recharged by fresh water. However, the regional 3D geometry of R4 would be needed to test this hypothesis. R4 is locally overlain by a thin low-permeability unit (late Pleistocene clays at the Expedition 313 sites; Miller et al., 2013b) possibly acting as a confining unit (Hathaway et al., 1979). Seawater might have penetrated into R4 where the

nonconsolidated sands forming R4 crop out on the outer shelf, or where the confining unit is breached by fluvial incisions (Lofi et al., 2013), such as the paleo–Hudson valley mapped on the middle shelf (Knebel et al., 1979). Incised valleys have also been recognized in the vicinity of the drill sites (Miller et al., 2013b).

In our 2D permeability model (Fig. 5B), R3 is disconnected from R4 by thin (<50 m) low-permeability units (C3b and C3c in M0028A; Table 3) and from R2 by a thick unit C3 (>170 m in M0027A; Table 3), making vertical connections improbable. However, due to the lateral variability of the clinoform geometries and of the sedimentary facies, some vertical or horizontal pore-water exchanges between R2, R3, and R4 can still be envisaged if reservoirs merge laterally.

At site 6011, drilled close to the coast, fresh water has been recovered in both fine-grained and coarse-grained deposits located deeper than 60 mbsf (Hathaway et al., 1976). While R2, R3, and R4 are saturated with salty water, the most proximal reservoir R1 contains fresh water (Fig. 5B). R1 probably forms the seaward extension of the onshore aquifers such as the Kirkwood-Cohansey aquifer system and the Atlantic City 800-foot sand, forming a major aquifer along the coast (Barton et al., 1993). In contrast to the reservoirs located farther offshore, the permeable layers there have not been salinized, and the connection with the other reservoirs remains an open question. Due to the complex architecture of the reservoirs at the margin scale, a 3D approach would be necessary to test this hypothesis, in order to determine the spatial variability of the geometry of the reservoirs.

### *Modern Water*

Two wells drilled 5.3 and 8.5 km offshore from Atlantic City (ACOW1 and ACOW2, Fig. 1) contain fresh water that has been radiocarbon dated as at least 22,000 $^{14}$C yr B.P. (and possibly 30,000 $^{14}$C yr B.P.) (McAuley et al., 2001), dating the water to at least the LGM in this area. These dates would support the hypothesis that the fresh water sampled at the Expedition 313 drilling sites is fossil. However, van Geldern et al. (2013) suggested that these radiocarbon ages might be overestimated. Moreover, these ages are not supported by oxygen and hydrogen stable isotope measurements performed on pore waters at the Expedition 313 drilling sites (van Geldern et al., 2013). Van Geldern et al. (2013) did not find any evidence for old emplacement by meteoric recharge during Pleistocene sea-level lowstands and onshore subglacial recharge. Instead, the isotopic data suggest that the fresh-water intervals are recharged by meteoritic waters that are either modern, or were formed under climatic and hydrologic conditions similar to modern conditions. Waters recharged during the LGM are usually recognized worldwide by depletion in δD and $\delta^{18}$O in comparison to Holocene groundwater (Clark and Fritz, 1997). However, according to Plummer (1993), paleowaters of the Floridian aquifer systems that recharged during the LGM are enriched compared to the local Holocene groundwater and isotopic interpretations therefore remain subject to caution. Keeping these uncertainties in mind, we discuss whether the presence of modern water in C1–C3 (and R4) could be compatible, from a geometrical point of view, with our 2D permeability model (Fig. 5B).

Stable isotope data of the pore water in Hole M0027A and in Hole M0029A indicate a mixing line between onshore groundwater recharge and modern seawater (van Geldern et al., 2013). As suggested by van Geldern et al. (2013), this situation could reflect an interplay of active recharge from onshore and seawater intrusion. The low-permeability units C1 and C3 are similar in thickness, dip gently seaward, and are connected near the coast with R1 (saturated with fresh water). Such geometry is compatible with a present-day connection to the land and a recharge by fresh water if onshore hydraulic heads are high enough to drive modern meteoric water offshore. Vertical hydraulic gradients are unknown in C1 and C3, but in terms of grain size and geometry, active flows cannot be excluded. Although units C1 and C3 are expected to have a low permeability, they are not expected to be impermeable as they are depleted in clays (Proust et al., 2010). For example, the fine-grained glaciolacustrine sediments on Nantucket Island have a low permeability ($k$ = 1 mD) similar to that of our low-permeability units (blue shading in Fig. 5) and also contain Holocene meteoric water (Person et al., 2012). Simple 1D advection-dispersion models showed that advection is the dominant fluid transport mechanism within these deposits and indicate that remnants of Pleistocene glacial melt water could be flushed in <200 yr (Person et al., 2012).

If active flows occur in the low-permeability units, some would also be expected in the permeable units forming the reservoirs R2–R4, if these are also connected to the land. The reservoirs are likely to be geometrically connected to each other and to the modern seafloor. The presence of salt water in these reservoirs can thus tentatively be explained by seawater penetration as a result of fast density-driven flow in these units where $k$ is orders of magnitude greater than in the low-permeability units. In this case, we would expect the vertical flow to be greater relative to any horizontal land to sea directed flow within the connected reservoirs.

In R4, the fresh-water layers or lenses are surrounded by permeable sands saturated with salt water (Fig. 5B). The fine-grained layers bearing the fresh water are currently geometrically disconnected from the land and from each other. This 2D geometry is hardly compatible with a modern recharge from the continent and would instead suggest that the clayey intervals internal to R4 contain a fresh-water remnant from older hydrological events (likely the last lowstand phase). However, the 3D spatial extension and connectivity of these layers is needed to confirm this interpretation.

## CONCLUSIONS

The salinity distribution in a reservoir strongly relies on the interaction between groundwater fluid dynamics and the geological environment, which is commonly complex and anisotropic. The spatial distribution (at several scales) of porosity, hydraulic conductivity, and other hydraulic parameters in the subsurface are thus of major importance, and are strongly related to both geological context and to depositional processes at geological time scales. Expedition 313 offers a unique opportunity to access the internal structure of a siliciclastic system, and to refine our knowledge of how the geological heterogeneity can affect groundwater exchanges at the scale of a passive margin. A key aspect of this study is its multiscale nature alongside a multidisciplinary approach combining seismic profiles, geochemical, core, petrophysical, and logging data. This approach enables both scale and heterogeneity problems in a porous aquifer to be evaluated.

### Salinity Distribution Beneath the Middle Shelf

For the majority of the successions drilled, the organization of the reservoirs is multilayered, with fresh water (salinity < 15 g/L) intervals alternating vertically with salty intervals (salinity > 15 g/L) of varied thicknesses.

Fresh water is preferentially stored in fine-grained and low-permeability deposits, whereas salty waters are recovered in coarse-grained and high-permeability units. The processes controlling fluid distribution are permeability related.

Cemented intervals are observed at some fresh water–salt water boundaries, forming permeability barriers or relative obstacles to fluid flow.

In the deepest part of holes M0028A and M0029A, the salinity varies independently of porosity and lithology, suggesting advection-diffusion of deep-rooted brines upwelling from depth.

## Reservoir Architecture and Permeability Distribution

One difficulty in offshore groundwater flow modeling is determining which structure to put into the model, since aquifers are invisible from the surface and geological information is scarce. We have built a 2D model of reservoir geometry and permeability distribution along a dip transect of the margin, extrapolated from combined clinoform geometries observed in seismic data and sedimentary facies described from cores. This model clearly illustrates the importance of taking into account the spatial heterogeneity of geological system at several scales.

Lithology reflects permeability at a small scale, whereas seismic facies and system tracts can be used to infer the reservoir geometry at a larger scale.

Four main reservoirs (high-permeability units R1–R4) that are relatively disconnected (on the dip section presented) have been identified. These are essentially developed in coarse-grained deposits observed either in some clinoform topsets (R4), in upper foresets (R2, R3), or in both of them (R1).

Reservoirs R2–R4 contain salty water, while the most proximal reservoir R1, located close to the coastline, is saturated with fresh water, and may form the seaward extension of onshore aquifer.

Each of these four reservoirs is separated by low-permeability units (C1–C4) of varied thicknesses and relatively broad spatial extension. Excluding those intervals under brine influence, these units contain fresh water. Unit C3, located in the fine-grained deposits of some certain clinoform topsets, is geometrically laterally connected to the shore.

The proposed geometries are of primary importance when considering the possible emplacement mechanisms for these waters. Coupling our 2D permeability model with porewater salinities allows us to discuss the possible pathways for the fresh and salty water below the New Jersey shelf.

Post-LGM density driven flows are the likely origin of the salty water contained in the distal reservoirs (R2–R4). Complex present-day vertical or horizontal connections among the reservoirs are probable in 3D with the modern seafloor as an end member, and possibly the shallow onshore aquifers as another.

At the Expedition 313 drilling sites, the fresh waters stored in C1–C3 have a postdepositional age. Our 2D permeability model alone does not allow the discrimination of whether these waters are modern (van Geldern et al., 2013) or paleowaters (Hathaway et al., 1979; Kohout et al., 1988). From a geometrical point of view, C1 and C3 are connected to the land; this is compatible with a present-day onshore recharge. Our 2D model, however, suggests that the fresh-water lenses contained in R4 are more easily explained by a fossil origin (Pleistocene lowstands?).

Further work must be done to clarify the emplacement mechanisms. A 3D approach would be necessary to refine our knowledge of the lateral variability of the reservoir geometry, which can have a considerable impact on both groundwater pathways and dynamics. In order to test the specific flow processes that are active in this environment, future studies will benefit from the inclusion of our 2D permeability model in a groundwater model. The approach developed in this study would be valuable for other margins where borehole salinity data are available.

### ACKNOWLEDGMENTS

This research used samples and data provided by the Integrated Ocean Drilling Program (IODP) and the International Continental Scientific Drilling Program (ICDP). We acknowledge the two anonymous reviewers and the editor for constructive comments on the first version of the manuscript. We thank R. van Geldern and P. Gouze for useful discussions.

### REFERENCES CITED

Archie, G.E., 1942, The electrical resistivity log as an aid in determining some reservoir characteristics: American Institute of Mining and Metallurgical Engineers Transactions, v. 146, p. 54–61, doi:10.2118/942054-G.

Austin, J.A.J., Christie-Blick, N., and Malone, M.J., 1998, Proceedings of the Ocean Drilling Program, Initial reports, Volume 174A: College Station, Texas, Ocean Drilling Program, doi:10.2973/odp.proc.ir.174A.1998.

Barlow, P.M., 2003, Ground water in freshwater-saltwater environments of the Atlantic Coast: U.S. Geological Survey Circular 1262, 113 p., http://pubs.usgs.gov/circ/2003/circ1262/.

Barton, G.J., Storck, D.A., and Paulachok, G.N., 1993, Records of wells, exploratory boreholes, and groundwater quality, Atlantic county and vicinity, New Jersey, Trenton, N.J.: U.S. Geological Survey Open-File Report 92-631, 95 p.

Bear, J., 1971, Dynamics of fluids in porous media: New York, Dover Publications, 784 p.

Bear, J., Cheng, A.H.-D., Sorek, S., and Ouazar, D.H.I., eds., 1999, Seawater intrusion in coastal aquifers—Concepts, methods, and practices: Dordrecht, Kluwer Academic Publishers, 631 p.

Berner, R.A., 1980, Early diagenesis: A theoretical approach: Princeton, New Jersey, Princeton University Press, 241 p.

Bloomfield, J.P., and Williams, A.T., 1995, An empirical liquid permeability–gas permeability correlation for use in aquifer properties studies: Engineering Geology Quarterly Journal, v. 28, p. s143–s150, doi:10.1144/GSL.QJEGH.1995.028.S2.05.

Bowling, J.C., Rodriguez, A.B., Harry, D.L., and Zheng, C., 2005, Delineating alluvial aquifer heterogeneity using resistivity and GPR data: Ground Water, v. 43, p. 890–903, doi:10.1111/j.1745-6584.2005.00103.x.

Bugna, G.C., Chanton, J.P., Cable, J.E., Burnett, W.C., and Cable, P.H., 1996, The importance of groundwater discharge to the methane budgets of nearshore and continental shelf waters of the northeastern Gulf of Mexico: Geochimica et Cosmochimica Acta, v. 60, p. 4735–4746, doi:10.1016/S0016-7037(96)00290-6.

Burnett, W.C., Taniguchi, M., and Oberdorfer, J., 2001, Measurement and significance of the direct discharge of groundwater into the coastal zone: Journal of Sea Research, v. 46, p. 109–116, doi:10.1016/S1385-1101(01)00075-2.

Clark, I., and Fritz, P., 1997, Environmental isotopes in hydrology: Boca Raton, Florida, CRC Press, 328 p.

Cohen, D., and 12 others, 2010, Origin and extent of fresh paleowaters on the Atlantic continental shelf, USA: Ground Water, v. 48, p. 143–158, doi:10.1111/j.1745-6584.2009.00627.x.

Cossé, R., 1993, Basics of reservoir engineering: Paris, Editions Technip, 372 p.

Dugan, B., and Flemings, P.B., 2000, Overpressure and fluid flow in the New Jersey continental slope: Implications for slope failure and cold seeps: Science, v. 289, p. 288–291, doi:10.1126/science.289.5477.288.

Ellis, D.V., and Singer, J.M., eds., 2007, Well logging for earth scientists (second edition): Berlin, Springer, 692 p.

Faure, H., Walter, R.C., and Grant, D.R., 2002, The coastal oasis: Ice age springs on emerged continental shelves: Global and Planetary Change, v. 33, p. 47–56, doi:10.1016/S0921-8181(02)00060-7.

Fleury, P., Bakalowicz, M., and De Marsily, G., 2007, Submarine springs and coastal karst aquifers: A review: Journal of Hydrology, v. 339, p. 79–92, doi:10.1016/j.jhydrol.2007.03.009.

Groen, J., Velstra, J., and Meesters, A.G.C.A., 2000, Salinization processes in paleowaters in coastal sediments of Suriname: Evidence from $\delta^{37}$Cl analysis and diffusion modeling: Journal of Hydrology, v. 234, p. 1–20, doi:10.1016/S0022-1694(00)00235-3.

Hathaway, J.C., Schlee, J.S., Poag, C.W., Valentine, P.C., Weed, E.G.A., Bothner, M.H., Kohout, F.A., Manheim, F.T., Schoen, R., Miller, R.E., and Schultz, D.M., 1976, Preliminary summary of the 1976 Atlantic Margin Coring Project of the U.S. Geological Survey: U.S. Geological Survey Open-File Report 76-844, 217 p.

Hathaway, J.C., Poag, C.W., Valentine, P.C., Miller, R.E., Schultz, D.M., Mannheim, F.T., Kohout, F.A., Bothner, M.H., and Sangrey, D.A., 1979, U.S. Geological Survey core drilling on the Atlantic Shelf: Science, v. 206, p. 515–527, doi:10.1126/science.206.4418.515.

Inwood, J., Lofi, J., Bjerrum, C.J., Basile, C., Otsuka, H., Valppu, H., Mountain, G., and Proust, J., and the Expedition 313 Scientists, 2010, Statistical classification of log response as an indicator of facies variation during changes in sea level: IODP Exp 313: American Geophysical Union, Fall Meeting 2010, abs. PP11E–1462.

Inwood, J., Lofi, J., Davies, S., Basile, C., Bjerum, C., Mountain, G., Proust, J.-N., Otsuka, H., and Valppu, H., 2013, Statistical classification of log response as an indicator of facies variation during changes in sea level: Integrated Ocean Drilling Program Expedition 313: Geosphere, v. 9, doi:10.1130/GES00913.1.

Klinkenberg, L.J., 1941, The permeability of porous media to liquids and gases, *in* Drilling and production practice 1941: Washington, D.C., American Petroleum Institute, p. 200–213.

Knebel, H.J., Wood, S.A., and Spiker, E.C., 1979, Hudson River: Evidence for extensive migration on the exposed continental shelf during Pleistocene time: Geology, v. 7, p. 254–258, doi:10.1130/0091-7613(1979)7<254:HREFEM>2.0.CO;2.

Kohout, F.A., Hathaway, J.C., Folger, D.W., Bothner, M.H., Walker, E.H., Delaney, D.F., Frimpter, M.H., Weed, E.G.A., and Rhodehamel, E.C., 1977, Fresh groundwater stored in aquifers under the continental shelf: Implications from a deep test, Nantucket Island, Massachusetts: Water Resources Bulletin, v. 13, p. 373–386, doi:10.1111/j.1752-1688.1977.tb02031.x.

Kohout, F.A., Meisler, H., Meyer, F.W., Johnston, R., Leve, G., and Wait, R., 1988, Hydrogeology of the Atlantic continental margin, *in* Sheridan, R.E., and Grow, J.A., eds., The Atlantic continental margin: Boulder, Colorado, Geological Society of America, Geology of North America, v. I-2, p. 463–480.

Kooi, H., and Groen, J., 2000, Modes of seawater intrusion during transgressions: Water Resources Research, v. 36, p. 3581–3589, doi:10.1029/2000WR900243.

Kooi, H., and Groen, J., 2001, Offshore continuation of coastal groundwater systems; predictions using sharp-interface approximations and variable-density flow modeling: Journal of Hydrology, v. 246, p. 19–35, doi:10.1016/S0022-1694(01)00354-7.

Kooi, H., and Groen, J., 2003, Geological processes and management of groundwater resources in coastal areas: Geologie en Mijnbouw, v. 82, p. 31–40.

Land, L.A., and Paul, C.K., 2000, Submarine karst rimming the continental slope in the Straits of Florida: Geo-Marine Letters, v. 20, p. 123–132, doi:10.1007/s003670000041.

Li, Y.H., and Gregory, S., 1974, Diffusion of ions in sea water in deep-sea sediments: Geochimica et Cosmochimica Acta, v. 88, p. 708–714, doi:10.1016/0016-7037(74)90145-8.

Lofi, J., Berné, S., Tesson, M., Séranne, M., and Pezard, P., 2012, Giant solution-subsidence structure in the Western Mediterranean related to deep substratum dissolution: Terra Nova, v. 24, p. 181–188, doi:10.1111/j.1365-3121.2011.01051.x.

Lofi, J., Pezard, P., Bouchette, F., Raynal, O., Denchik, N., Levannier, A., Dezileau, L., and Certain, R., 2013, Integrated onshore-offshore investigation of a Mediterranean layered coastal aquifer: Ground Water, doi:10.1111/j.1745-6584.2012.01011.x.

Malone, M.J., and Martin, J.B., 2000, Data report: Isotopic composition of pore fluids, New Jersey shelf and slope, *in* Christie-Blick, N., et al., eds., Proceedings of the Ocean Drilling Program, Scientific results, Volume 174A: College Station, Texas, Ocean Drilling Program, p. 1–11, doi:10.2973/odp.proc.sr.174a.156.2000.

Malone, M.J., Claypool, G., Martin, J.B., and Dickens, G.R., 2002, Variable methane fluxes in shallow marine systems over geologic time: The composition and origin of pore waters and authigenic carbonates on the New Jersey shelf: Marine Geology, v. 189, p. 175–196, doi:10.1016/S0025-3227(02)00474-7.

Manheim, F.T., and Paull, C.K., 1981, Patterns of groundwater salinity changes in a deep continental-oceanic transect off the southeastern Atlantic coast of the U.S.: Journal of Hydrology, v. 54, p. 95–105, doi:10.1016/0022-1694(81)90154-2.

Marksamer, A.J., Person, M.A., Day-Lewis, F.D., Lane, J.W., Jr., Cohen, D., Dugan, B., Kooi, H., and Willet, M., 2007, Integrating geophysical, hydrochemical, and hydrologic data to understand the freshwater resources on Nantucket Island, Massachusetts, *in* Hyndman, D.W., et al., eds., Subsurface hydrology: Data integration for properties and processes: American Geophysical Union Monograph 171, p. 143–159, doi:10.1029/171GM12.

McAuley, S., Barringer, J.L., Paulachok, G.N., Clark, J.S., and Zapecza, O.S., 2001, Ground-water flow and quality in the Atlantic City 800-foot sand, New Jersey: New Jersey of Environmental Protection Geological Survey Report GSR 41, 86 p.

McHugh, C.M., Hartin, C.A., Mountain, G.S., and Gould, H.M., 2010, The role of glacio-eustasy in sequence formation: Mid-Atlantic continental margin, USA: Marine Geology, v. 277, p. 31–47, doi:10.1016/j.margeo.2010.08.009.

Meisler, H., Leahy, P.P., and Knobel, L., 1984, Effect of eustatic sea-level changes on saltwater-freshwater in the northern Atlantic Coastal Plain: U.S. Geological Survey Water-Supply Paper 2255, 34 p.

Miller, K.G., and Snyder, S.W., 1998, Proceedings of the Ocean Drilling Program, Scientific results, Volume 150X: College Station, Texas, Ocean Drilling Program, doi:10.2973/odp.proc.sr.150x.1997.

Miller, K.G., Sugarman, P., Van Fossen, M., Liu, C., Browning, J.V., Queen, D., Aubry, M.-P., Burckle, L.D., Goss, M., and Bukry, D., 1994, Island Beach site report, Proceedings of the Ocean Drilling Program, Initial reports, Volume 150X: College Station, Texas, Ocean Drilling Program, p. 5–33, doi:10.2973/odp.proc.ir.150x.111.1994.

Miller, K.G., Browning, J.V., Mountain, G.S., Bassetti, M.A., Monteverde, D., Katz, M.E., Inwood, J., Lofi, J., and Proust, J.N., 2013a, Sequence boundaries are impedance contrasts: Core-seismic-log integration of Oligocene-Miocene sequences, New Jersey shallow shelf: Geosphere, v. 9, doi:10.1130/GES00858.1.

Miller, K.G., Sugarman, P.J., Browning, J.V., Sheridan, R.E., Kulhanek, D.K., Monteverde, D.H., Wehmiller, J.F., Lombardi, C., and Feigenson, M.D., 2013b, Pleistocene sequence stratigraphy of the shallow continental shelf, offshore New Jersey: Constraints of Integrated Ocean Drilling Program Leg 313 core holes: Geosphere, v. 9, p. 74–95, doi:10.1130/GES00795.1.

Monteverde, D.H., 2008, Sequence stratigraphic analysis of early and middle Miocene shelf progradation along the New Jersey margin: New Brunswick, New Jersey, Rutgers University, 263 p.

Mountain, G.S., Miller, K.G., Blum, P., et al., 1994, Proceedings of the Ocean Drilling Program, Initial reports, Volume 150: College Station, Texas, Ocean Drilling Program, doi:10.2973/odp.proc.ir.150.1994.

Mountain, G.S., Proust, J.-N., McInroy, D., and Cotterill, C., and the Expedition 313 Scientists, 2010, Proceedings of the Integrated Ocean Drilling Program, Volume 313: Tokyo, Integrated Ocean Drilling Program Management International, Inc., doi:10.2204/iodp.proc.313.2010.

Mullikin, L.G., 1990, Records of selected wells in Atlantic County, New Jersey: New Jersey Department of Environmental Protection, Division of Water Resources, Geological Survey Report 22, 82 p.

Person, M., Dugan, B., Swenson, J.B., Urbano, L., Stott, C., Taylor, J., and Willet, M., 2003, Pleistocene hydrology of the Atlantic continental shelf, New England: Geological Society of America Bulletin, v. 115, p. 1324–1343, doi:10.1130/B25285.1.

Person, M., Marksamer, A.J., Sauer, P., Brown, K., Bish, D., Litch, L., Dugan, B., Krothe, N., and Willet, M., 2012, Use of a vertical $\delta^{18}O$ profile to constrain hydraulic properties and recharge rates across a glacio-lacustrine unit, Nantucket Island, Massachusetts, USA: Hydrogeology Journal, v. 20, p. 325–336, doi:10.1007/s10040-011-0795-1.

Plummer, L.N., 1993, Stable isotope enrichment in paleowaters of the southeast Atlantic coastal plain, United States: Science, v. 26, p. 2016–2220.

Proust, J., Mountain, G., Ando, H., Browning, J.V., Hesselbo, S.P., Hodgson, D.M., Rabineau, M., and Sugarman, P., and the Expedition 313 Scientists, 2010, Sea-level controls on the sediment architecture of the US New jersey passive margin during Oligocene and Miocene times: IODP Expedition 313 preliminary results: American Geophysical Union, Fall Meeting 2010, abs. PP13F–01.

Revil, A., and Cathles, L.M., III, 1999, Permeability of shaly sands: Water Resources Research, v. 35, p. 651–662, doi:10.1029/98WR02700.

Robb, J.M., 1984, Spring sapping on the lower continental slope, offshore New Jersey: Geology, v. 12, p. 278–282, doi:10.1130/0091-7613(1984)12<278:SSOTLC>2.0.CO;2.

Salvati, R., and Sasowsky, I., 2002, Development of collapse sinkholes in areas of groundwater discharge: Journal of Hydrology, v. 264, p. 1–11, doi:10.1016/S0022-1694(02)00062-8.

Sanders, L.L., 1998, A manual of field hydrogeology: New York, Prentice Hall, 381 p.

Schlee, J.S., and Fritsch, J., 1982, Seismic stratigraphy of the Georges Bank Basin complex offshore New England: Rifted margins: Field investigations of margin structure and stratigraphy, *in* Watkins, J.S., and Drake, C.L., eds., Studies in continental margin geology: American Association of Petroleum Geologists Memoir 34, p. 223–251.

Scientific Committee on Oceanic Research, Land-Ocean Interactions in the Coastal Zone, 2004, Submarine groundwater discharge: Management implications, measurements and effects (IHP-VI Series on groundwater 5, IOC manuals and guides 44): Paris, United Nations Educational, Scientific and Cultural Organization, 35 p.

Serra, O., 1984, Fundamentals of well-log interpretation: Amsterdam, Netherlands, Elsevier, 423 p.

Sultan, N., Cochonat, P., Bourillet, J.-F., and Cayocca, F., 2001, Evaluation of the risk of marine slope instability: A pseudo-3D approach for application to large areas: Marine Georesources and Geotechnology, v. 19, p. 107–133.

Swarzenski, P.W., Reich, C.D., Spechler, R.M., Kindinger, J.L., and Moore, W.S., 2001, Using multiple geochemical tracers to characterize the hydrogeology of the submarine spring off Crescent Beach, Florida: Chemical Geology, v. 179, p. 187–202, doi:10.1016/S0009-2541(01)00322-9.

Szabo, Z., Keller, E.A., and Defawe, R.M., 2006, Porewater quality in the clay-silt confining units of the Lower Miocene Kirkwood Formation and hypothetical effects on water quality in the Atlantic City 800-Foot Sand, northeastern Cape May County, New Jersey, 2001: U.S. Geological Survey Scientific Investigations Report 2006-5134, 26 p.

Taniguchi, M., Burnett, W.C., Cable, J.E., and Turner, J.V., 2002, Investigation of submarine groundwater discharge: Hydrological Processes, v. 16, p. 2115–2129, doi:10.1002/hyp.1145.

Tanikawa, W., and Shimamoto, T., 2006, Klinkenberg effect for gas permeability and its comparison to water permeability for porous sedimentary rocks: Hydrology and Earth System Sciences Discussions, v. 3, p. 1315–1338, doi:10.5194/hessd-3-1315-2006.

Toth, D.J., and Lerman, A., 1975, Stratified lake and oceanic brines: Salt movement and time limits of existence: Limnology and Oceanography, v. 20, p. 715–728, doi:10.4319/Lo.1975.20.5.0715.

van Geldern, R., Hayashi, T., Böttcher, M.E., Mottl, M.J., Barth, J.A.C., and Stadler, S., 2013, Stable isotope geochemistry of pore waters and marine sediments from the New Jersey shelf: Methane formation and fluid origin: Geosphere, v. 9, p. 96–112, doi:10.1130/GES00859.1.

Vernet, R., 2000, Karst et hydrocarbures. Rospo mare: un paleokarst pétrolier exploité en mer Adriatique (Italie): Geochronique, v. 76, p. 34–35.

Watts, A.B., and Steckler, M.S., 1979, Subsidence and eustasy at the continental margin of eastern North America, *in* Talwani, M., et al., eds., Deep drilling results in the Atlantic Ocean: Continental margins and paleoenvironment: American Geophysical Union Maurice Ewing Series Volume 3, p. 218–234.

Withjack, M.O., and Schlische, R.W., 2005, A review of tectonic events on the passive margin of eastern North America, *in* Post, P. J., et al., eds., Petroleum systems of divergent continental margin basins (Proceedings of the 25th Annual GCSSEPM Foundation Bob F. Perkins Research Conference): Gulf Coast Section, SEPM (Society for Sedimentary Geology) Publication 025, p. 203–235.

Withjack, M.O., Schlische, R.W., and Olsen, P.E., 2012, Development of the passive margin of eastern North America: Mesozoic rifting, igneous activity, and breakup, *in* Bally, A.W., and Roberts, D.G., eds., Principles of Phanerozoic regional geology, Volume 1: Amsterdam, Netherlands, Elsevier, p. 301–335.